Journal of Hydrology: Regional Studies 9 (2017) 48–68

Contents lists available at ScienceDirect

Journal of Hydrology: Regional Studies

journal homepage: www.elsevier.com/locate/ejrh

Uncertainty based assessment of dynamic freshwater scarcity in semi-arid watersheds of Alberta, Canada

Monireh Faramarzi[a,*], Karim C. Abbaspour[b], W.L. (Vic) Adamowicz[c], Wei Lu[c], Jon Fennell[d], Alexander J.B. Zehnder[e], Greg G. Goss[f]

[a] Department of Earth and Atmospheric Sciences, Faculty of Science, University of Alberta, Alberta, Canada
[b] Eawag, Swiss Federal Institute of Aquatic Science and Technology, Duebendorf, Switzerland
[c] Department of Resource Economics and Environmental Sociology, University of Alberta, Alberta, Canada
[d] Department of Renewable Resources, University of Alberta, Integrated Sustainability Consultants Ltd., Alberta, Canada
[e] Nanyang Technological University (NTU), Sustainable Earth Office, Singapore 637459, Singapore
[f] Department of Biological Sciences, Faculty of Science, University of Alberta, Alberta, Canada

ARTICLE INFO

Article history:
Received 6 May 2016
Received in revised form
25 November 2016
Accepted 25 November 2016

Keywords:
Hydrological modeling
Blue water scarcity
Groundwater stress
Irrigated wheat yield
Uncertainty analysis

ABSTRACT

Study region: Alberta, Canada.
Study focus: The security of freshwater supplies is a growing concern worldwide. Understanding dynamics of water supply and demand is the key for sustainable planning and management of watersheds. Here we analyzed the uncertainties in water supply of Alberta by building an agro-hydrological model, which accounts for major hydrological features, geo-spatial heterogeneity, and conflicts over water-food-energy resources. We examined the cumulative effects of natural features (e.g., potholes, glaciers, climate, soil, vegetation), anthropogenic factors (e.g., dams, irrigation, industrial development), environmental flow requirements (EFR), and calibration schemes on water scarcity in the dynamics of blue and green water resources, and groundwater recharge.
New hydrological insights for the region: Natural hydrologic features of the region create a unique hydrological system, which must be accurately represented in the model for reliable estimates of water supply at high spatial and temporal resolution. Accounting for EFR, increases the number of months of water scarcity and the population exposed. Severe blue water scarcity in spring and summer months was found to be due to irrigated agriculture, while in winter months it was mostly due to the demands of petroleum or other industries. We found over exploitation of the groundwater in southern subbasins and concluded that more detailed analysis on groundwater flow and connectivity is required. Our study provides a general and unified approach for similar analyses in other jurisdictions around the world.

1. Introduction

Understanding temporal and spatial dynamics of water scarcity is key for sustainability of freshwater supplies. Economic expansion, population growth, extended environmental concerns, and climate change are increasing surface water scarcity and depleting groundwater resources threatening the sustainability of the natural ecosystem and human activities (Beek

* Corresponding author.
E-mail address: monireh.faramarzi@ualberta.ca (M. Faramarzi).

http://dx.doi.org/10.1016/j.ejrh.2016.11.003

et al., 2011; Doll, 2009; Famiglietti, 2014; Mwangi et al., 2016; Oki and Kanae, 2006). Global organizations and national governments have announced water stress as the largest global risk and the main reason for regional insecurity (Intelligence Community Assessment (ICA), 2012; World Economic Forum, 2015). To manage limited water resources, development plans have been shifted from a sector specific focus to a broader scale through integrated measures (UNEP, 2011). The studies on integrated water resources management have mostly been concerned with sustainability issues aiming to understand the balance between supply and demand components (Alcamo et al., 2007; Richey et al., 2015). The water-food-energy nexus is considered as an emerging concept that advocates sustainable management of the water-food-energy system in concert with environmental protection (Vlotman and Ballard, 2014). Within the context of water and food sustainability, the majority of research studies have focused on understanding the role of a virtual water trade strategy and agricultural water management in alleviating groundwater and surface water scarcity at the global (Allan, 1997; Chapagain et al., 2006; Lenzen et al., 2013; Yang et al., 2006), regional (Zeitoun et al., 2010), and national (Faramarzi et al., 2010a; Talozi et al., 2015) scales. To determine levels of sustainable water use, and to warrant balance between water supply and demand, it is critical to understand the spatial and temporal dynamics of water scarcity and the hydrologic system with its associated physical processes.

Water scarcity analysis is useful to understand the balance between water supply and water demand (Hoekstra et al., 2012) that helps to manage human interaction with natural systems. Different approaches have been developed to assess water stress worldwide. These are: i) the per-capita water availability indicator (Falkenmark et al., 1989), ii) the critical ratio indicator (Alcamo et al., 2003), iii) the International Water Management Institute (IWMI) indicator (Seckler et al., 1998), and iv) the water poverty index (Sullivan et al., 2003). Given the widespread use of these indicators, their accuracy depends on the accuracy of the water supply and demand assessments. Here we refer to some shortcomings in the assessment of water supply and demand terms that has resulted in an inaccurate representation of the water scarcity in large-scale studies:

1.1. Water supply

Given that water is a dynamic and complex factor whose availability and variability of supply depends on both natural features and human factors (Richey et al., 2015), it is essential to utilize hydrological models as tools to systematically assess water availability and scarcity. Global hydrological models have been applied to simulate dynamic water resources at national, river basin, and recently at 0.5° grid resolutions (Alcamo et al., 2003; Beek et al., 2011; Feketa and Vorosmarty 2002; Oki and Kanae 2006). They have also been used to estimate surface and groundwater scarcity at high spatial and monthly temporal resolution (e.g., Beek et al., 2011; Richey et al., 2015; Wada et al., 2011). Although most models provide critical information at the global scale, often they are prone to poor representation of the actual physical processes at the local level where most of the decisions around water management are being made. High-resolution global studies often suffer from data scarcity and model complexity when dealing with the model building, calibration, and validation processes (Clark et al., 2015; Nazemi and Wheater, 2015; Wheater and Gober, 2013). Abovementioned global models often are only calibrated and validated against long-term annual discharges; hence providing a poor temporal resolution. Often they are modified using a correction factor to offset the errors in the temporal and spatial patterns, resulting in an inconsistent water balance. The most sophisticated studies have been validated using time series data of a few hydrometric stations on outlets of large river basins. In addition, most of the large-scale studies use globally reconstructed climate data without qualifying their hydrological responses at a regional level. Overlooking these details, negatively affects simulation of the hydrological processes at a high grid resolution, thereby reducing reliability at the local level.

The regional and river basin studies on water scarcity analysis have utilized more locally representative data for hydrologic model setup and calibration (e.g., Graveline et al., 2014; He and Hogue, 2012; Neverre et al., 2016). However, simulation of distributed physical processes are often simplified, and time-variant representation of the spatial patterns are compromised by ignoring an adequate calibration and validation of the models in studies of water supply and water scarcity at the regional level (Beck and Bernauer, 2011; Gain and Giupponi 2015; Sušnik et al., 2012).

1.2. Water demand

Previous studies used national water withdrawal statistics that are often static values representing water use of an entire country (Vörösmarty et al., 2000). The main drawback with withdrawal statistics is their poor spatial and temporal resolution, as well as ignoring of the return flow to the hydrological system, which becomes available for use in downstream watersheds (Kijne et al., 2003). Disregarding such important characteristics results in overestimation of water scarcity. More recent global scale studies assumed agriculture as the major water consumer, and utilized water balance models to account for dynamic water use of agricultural crops. However, to validate their model results they averaged their grid based model outputs to the national scale data and compared this with the available national average statistics (Mekonnen and Hoekstra, 2010) resulting in a poor representation of the actual water use over time and space. In addition, for sustainable management of the watersheds, there is an increasing interest to assess EFR to ensure health of aquatic ecosystem and the river's biodiversity (Vörösmarty et al., 2010). Recent studies used a simplistic approach and assumed 80% of total water availability for EFR, which does not change with river flow regime (Hoekstra et al., 2012). Limited studies used a monthly approach to account for river regime for the EFR to maintain various levels of habitat quality in the rivers (Liu et al., 2016; Tennant, 1976).

Alberta is a semi-arid province of western Canada. It is a province that encompasses many of the water security challenges faced worldwide. In Alberta, conflicts have already arisen in the context of water, food, energy, and environmental resources. Its economy depends on industries that rely heavily on sufficient and reliable quantities of good quality water. The province is globally recognized for its large petroleum production and agricultural exports. Allocation of 75% of the surface water withdrawal in northern basins of the province is devoted to oil and gas development, which has doubled since 2000 due to the expansion of production (Sauchyn et al., 2015). In addition, the province supplies large amounts of surface water for the production of diverse agricultural commodities and irrigated crops, which account for a large portion of agricultural exports from the country (See Fig. S1). Both have played an important role in the fast growing economy over the last few decades. While Alberta's economy and the well-being of its residents depend strongly on water, periodic water scarcity and flooding events pose serious economic, social, and environmental consequences for many areas of the province (GOA-Government of Alberta, 2010).

Our goal is to use Alberta as a case study to systematically assess dynamic freshwater availability and scarcity with a subbasin spatial and monthly temporal resolution that will provide a solid foundation for further assessment of water supply-demand challenges in the province. Our intention is to examine how simplification in water supply models and water demand data result in an over- or under-estimation of water availability and scarcity at regional and watershed scales. We aim to explicitly assess blue and green water components. Blue water is the liquid water in rivers, reservoirs, and ground water that is used in the production of commodities and allotted to economic goods and services (e.g., irrigated agriculture). It has both opportunity cost and environmental impacts. The green water flow is the total water vapour returned to the atmosphere by plants, and green water storage is the soil moisture that is a source of water for rainfed agriculture and ecosystem services (Falkenmark and Rockstrom, 2006). The heterogeneous hydro-climatic conditions and diverse management practices, in combination with the scarcity of data (especially in the northern remote areas and western mountainous region), make Alberta a unique and challenging example for understanding its hydrological system. The hydro-climatic system of Alberta encompasses most of the important challenges in hydrological modeling pertaining to hydrological processes, natural and anthropogenic factors such as data issues, climate variability, glaciers, dams, reservoirs, lakes, and irrigated agriculture. To the best of our knowledge a high resolution and province-wide hydrological model has not been developed for Alberta. Most of the previous studies in Alberta have been conducted at a catchment (e.g., Marshall, 2014) or river basin (e.g., Islam and Gan, 2014) scale.

For this project, we used the "Soil and Water Assessment Tool" (SWAT) (Arnold et al., 1998) since the program inherently lends itself easily to climate and landuse change analyses. We chose this program because: i) it integrates many related physical processes including hydrology, climate, snow, nutrient, soil, sediment, crop, pesticide, surface depressions (potholes), and agricultural and water management, ii) it has been successfully applied both worldwide (Abbaspour et al., 2015; Faramarzi et al., 2013; Gassman et al., 2007, 2010; Schierhorn et al., 2014) and in Canada (Shrestha et al., 2012; Seidou et al., 2012; Amon-Arma et al., 2013; Rahbeh et al., 2013; Trion and Caya 2014; Fu et al., 2014), iii) calibration and uncertainty analysis of the processes have been performed, and the related tools have been developed and continuously updated (Abbaspour, 2011).

Limitations of SWAT mostly occur within mountainous areas where glacier and snow melt dominate the flow process, and in wetland regions where wetland hydrology dominates water movement. Similarly, limitation occur in the non-spatial nature of hydrologic response units (HRU) within a subbasin, where the HRU is the smallest unit of SWAT water balance calculation, and in the areas of large water management activities where lack of data may inhibit proper characterization of the flow processes. Many of these issues, however, are currently being addressed and will be improved in the next version of SWAT.

In this research study we built two separate hydrological models of Alberta using SWAT to: (1) simulate detailed water supply processes including irrigated agriculture, and to calibrate and validate the model using monthly hydrometric data from 130 stations and irrigated wheat yields of 13 irrigated districts. In this scenario model (SM1) we provided prediction uncertainty in the assessment of water supply to address the errors related to heterogeneous hydro-climatic and geo-spatial conditions, diverse management practices, and scarce data in remote areas and mountainous regions; and (2) test the effects of process simplification and the single-outlet calibration scheme in accounting for water supply components. In this scenario model (SM2) we ignored simulation of irrigated agriculture, and calibrated the hydrological model using monthly discharges of the six outlets draining major watersheds in Alberta. Next, we compared the water scarcity indicators using the outputs of the two water supply models (SM1 and SM2), and water demand of various sectors with and without considering the EFR. Finally, we determined the sources of monthly blue water scarcity and areas of groundwater stress in different river basins.

2. Material and methods

2.1. Study area

Alberta is a semi-arid western province of Canada that has an area of about 660,000 km^2. Its altitude varies from 3747 m above sea level (masl) in the Rocky Mountains on the west side of the province to 152 masl in the northern basins. With a dry continental climate, large-scale climate anomalies originating from Pacific Ocean, cause the air temperature drop to as low as $-54\,^{\circ}C$ during the winter and rise as high as $40\,^{\circ}C$ during the summer (Lapp et al., 2013). Mean annual precipitation varies

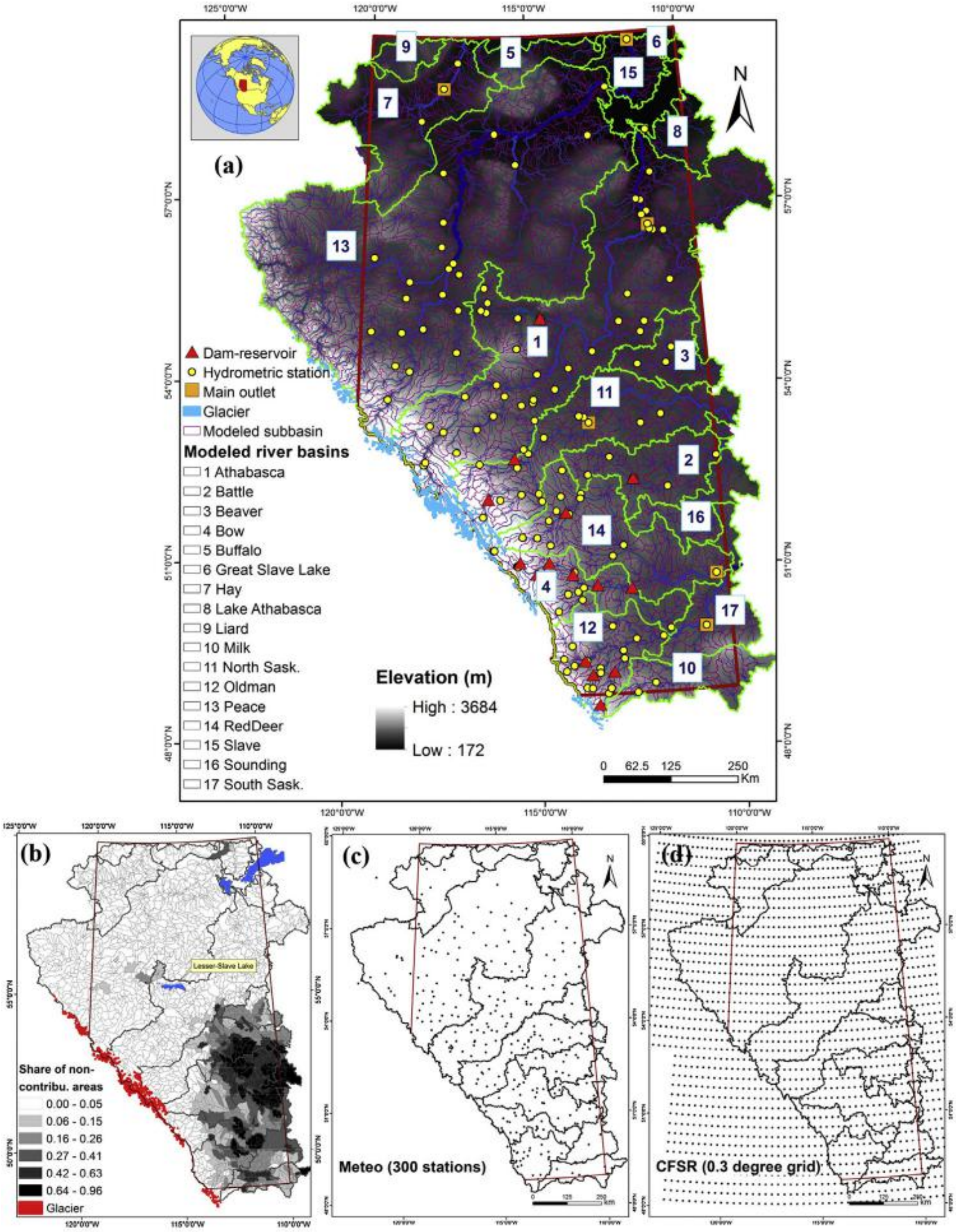

Fig. 1. Map of the modeled area illustrating the main river basins: (a) 130 hydrometric stations, dams-reservoirs and the modeled subbasins. Out of 130 hydrometric stations the six outlets depicted with orange squares are the far most downstream outlets where streamflow data represent upstream processes; (b) PFRA- Prairie Farm Rehabilitation Association non-contributing areas and the GLIMS- Global Land Ice Measurement from Space glacial regions; (c) meteorological stations (MS); and (d) Climate Forecast System Reanalysis (CFSR) grid points.

from 300 mm in the southeast to 600 mm or more in the foothills of the Rocky Mountains (ABENV- Alberta Environment, 2008; Mwale et al., 2009).

The province has 17 river basins with most of them originating from the snow melt dominated and glaciered highlands of the Rocky Mountains (ABENV, 2008). The 17 river basins are delineated in Fig. 1, while the characteristics of each river basin can be found in Tables S1 and S2. Most of the southern river basins are snow melt dominated in their upstream highland areas and glacier melt plays a major role in supplying downstream water needs in late summer. With 6% of Alberta's total water availability, the southern river basins (i.e., Bow, Oldman, and South Saskatchewan watersheds) provide nearly 57% of the irrigation water in Alberta. The landuse in the southern part of the province is primarily medium and large-scale agriculture; however, there is not enough rainfall and moisture to naturally sustain demands of agricultural crops in much of the region. As water scarcity is becoming a serious challenge in southern Alberta, actions are being taken to improve water conservation, efficiency of use, and productivity to meet water supply-demand constraints during periods of high water shortage. More details on the spatial pattern of economic activities and water challenges in the study area are provided in Table S2. The northern river basins generally originate from melting of perennial snow accumulations and glacier ice in the Rocky Mountains. The river flow regime reaches its minimum in winter months and its maximum in late spring and early summer, when snow and glacial melt waters from the river's head-waters combine with runoff from localized snow melt and rainfall throughout the basin. Most of the natural watersheds in the northern river basins are characterized by thick peat-rich soils with near-surface groundwater tables, which results in a significant amount of groundwater contributing to the river flows in the lowland areas (Eum et al., 2014). A large portion of the prairie landscape in the southern part of the province has a drainage network that is poorly developed resulting in many closed depressional areas referred to as "potholes" (Fig. 1b). This naturally undulating landscape influences the contribution of precipitation to streamflows as the depressions prohibit the direct drainage of surface runoff to the receiving stream. In southern Alberta, the landuse is primarily agricultural with thirteen organized irrigation districts. Substantial dams, diversion channels, off-stream reservoirs, and irrigation systems have been constructed to facilitate the provision of water for crop development in this region.

Overall, Alberta includes many of the water challenges identified worldwide. Modeling and understanding of the scientific and management challenges is critical not only for the sustainability of water supplies in Alberta, but also for addressing challenges of the dynamic, complex, and uncertain global water systems.

2.2. Water supply model scenarios: model setup, data, and calibration

SWAT2012 was used to simulate hydrological processes in Alberta. SWAT is a continuous-time and process-based hydrological model that solves hydrological water balance equation in the top soil layer (1–2m). Various modules are incorporated into the model to simulate natural and anthropogenic processes in watersheds including: climate, snow, standing water bodies (e.g., potholes and reservoirs), crop growth and crop water consumption, as well as others. On-stream dams and reservoirs can be treated as reservoirs located on the main streams that receive water from all upstream catchments. A water balance equation is solved to initiate water impoundment (e.g., potholes), which is a function of total inflow (e.g., runoff entering from the upstream subbasins, rainfall, groundwater contribution) and total outflow from the water bodies (e.g., evaporation, seepage into the subsurface). More details about the model are provided by Neitsch et al. (2011).

Data required to build the SWAT hydrological model of Alberta for SM1 and SM2 scenarios were obtained from various sources. These included: (i) digital elevation model (DEM) from the Shuttle Radar Topography Mission, with a 90 m resolution (Jarvis et al., 2008); (ii) landuse-land cover map from the GeoBase Land Cover Product (http://www.geobase.ca/geobase/en/data/landcover/csc2000v/description.html), which has a resolution of 30 m and distinguishes 36 landuse classes for Canada and 23 classes for our study area; (iii) soil map from the Agriculture Agri-Food Canada, Soil Landscapes of Canada V3.2 (http://sis.agr.gc.ca/cansis/nsdb/slc/index.html), which represents more than 90 soil classes for our study area; (iv) daily precipitation from 300 MS in Alberta (Fig. 1c) (http://climate.weather.gc.ca/); (v) daily minimum and maximum temperature, humidity, wind speed, and solar radiation from the National Centers for Environmental Prediction's CFSR (Fig. 1d) (http://globalweather.tamu.edu), which provides climate data at 0.3° grid resolution; (vi) map of natural surface impoundments (potholes) from the PFRA – Agriculture Agri-food Canada (AAFC, see Table S3), which includes the share of pothole area within each subbasin (Fig. 1b); (vii) daily operation of 15 large reservoirs/dams from Alberta Environment and Parks (AEP, formerly Alberta Environment and Sustainable Resource Development, AESRD); (viii) map of glaciers from the GLIMS (http://www.glims.org/); and (ix) monthly river discharge data from Environment Canada (http://www.ec.gc.ca/rhc-wsc/) for about 130 hydrometric stations.

A threshold area of 200 km^2 was used to discretize the province into 2255 subbasins. This threshold size of basin was selected to maintain a balance between the resolution of the available data, research objectives and resolution at which the outputs are required for post processing, and a practical SWAT project size. Dominant soil, landuse, and slope were considered in each subbasin. The daily operations of 15 large reservoirs/dams were incorporated in the model to better represent the downstream hydrological processes. Details on the climate data (Fig. 1c–d) are provided in Table S3. With this specification, the SM2 scenario model was calibrated only at the outlets of the six major watersheds where monthly river discharge data were best available (Fig. 1a). In conjunction with monthly river discharges of 130 stations (Fig. 1a), county based annual yields of spring-wheat was calibrated in SM1 scenario model to provide more confidence in the simulated evapotranspiration. The SWAT model uses climate variables, crop and soil parameters, management factors including dates of planting and harvesting, and volume of fertilizer use to simulate crop growth. For the simulation of irrigated wheat yield, which is the dominant water-intensive crop in Alberta, we used the auto-fertilization and auto-irrigation options of SWAT in SM1. Because of limited data availability on the date and amount of fertilizer and irrigation applications in each county for the study period, we used the auto-fertilization and auto-irrigation option of SWAT. This assumes an overall good management practices by the farmers. The crop-specific fertilizer application and ratio of nutrients (N:P:K) in each county was obtained from GOA (2004), where information on the use of fertilizers under various cropping and soil-climate conditions throughout the province is available. The required potential heat unit (PHU) for wheat to reach maturity is around 2000–2400 growing degree days in Alberta. We estimated yearly fluctuations of the PHU based on available temperature data. Other information including seasonal wheat ET, and dates of planting and harvesting were obtained from various sources within the GOA including Alberta Agriculture and Forestry (AAF, Table S3). It is worth mentioning that estimated ET by AAF is based on a detailed sub-county scale analysis, where the Food and Agriculture Organization Penman-Monteith equation (FAO, 1998) and locally derived crop coefficients are used. The ET data were not used as input to our model, but were used for verification of the simulated wheat ET in each county.

Potholes were activated in both scenario models (SM1 and SM2) using the PFRA map of non-contributing areas. Each subbasin with >10% non-contributing area was assigned a pothole. The most sensitive parameters were calibrated to represent spatial and temporal effects of the potholes on the downstream flow regime. Although the SWAT model is limited by the lumped parameterization of the spatial entities, and restricted in representing the hydrological connectivity and the 'spill-fill' processes (Evenson et al., 2015; Pomeroy et al., 2014), recent advancements in the model have dealt with some of these challenges making it a useful tool to represent geographically isolated wetlands and their relation to downstream hydrological behavior (Golden et al., 2014; Kiesel et al., 2010; Yang et al., 2010). To better handle snow and glacier melt, the glaciered subbasins were separated from non-glaciered subbasins and fine elevation bands were applied, where five snow parameters were adjusted for each band. With this level of parameterization the dynamics of snow/glacier melt were satisfactorily captured.

For calibration, validation, and uncertainty assessment the Sequential Uncertainty Fitting (SUFI-2) program (Abbaspour et al., 2004, 2007) was used. The program is linked to SWAT and provides the basis for parallel processing of multi-gauge calibration and large-scale parameterization schemes (Rouholahnejad et al., 2012). It also provides a platform for sensitivity and uncertainty analysis. We used the SUFI-2 program to calibrate and validate the model for the periods 1993–2007 and 1986–1992, respectively.

Based on an extensive SWAT literature review and authors' judgment, a total of 31 parameters, integrally related to streamflow, potholes, and crop growth were initially selected for a sensitivity analysis and tested using "one-at-a-time" and "global" sensitivity methods of the SWAT-CUP package (Abbaspour, 2011) for the study area (see Table S5). In SWAT-CUP one-at-a-time sensitivity analysis is performed to come up with reasonable ranges for the parameters. This analysis shows the response of a variable (e.g., discharge) to different values of a parameter when all other parameters are kept constant. We used the global sensitivity analysis to screen parameters and to determine the most influential parameters. This is important because parameters represent processes and we thereby identified the important processes to better focus on in a given region identified by a measured outlet (Abbaspour et al., 2004, 2007; Abbaspour, 2011). The sensitivity analysis is performed at every observed outlet. In a second step, these parameters were further differentiated by soil and land use type to depict the spatial variation of the system (i.e., SCS curve number CN2 of agricultural areas was assigned differently from that of forested areas). The use of stepwise regression sensitivity analysis outlined by Abbaspour (2011); Faramarzi et al. (2009); and Song et al. (2015) resulted in 109 sensitive parameters. We refer to these as the 'global' parameters. In this method parameter sensitivities are determined by calculating the following multiple regression system, which regresses the Latin hypercube generated parameters against the objective function values derived by the following equation:

$$g = \alpha + \sum_{i=1}^{m} \beta_i b_i \tag{1}$$

where g is the goal function and b_i is the parameter. A t-test is then used to identify the relative significance of each parameter b_i. The sensitivities given above are estimates of the average changes in the objective function resulting from changes in each parameter, while all others are changing. This gives relative sensitivities based on linear approximations and, hence, only provides partial information about the sensitivity of the objective function to model parameters. In this analysis, the larger the value of t-stat (in absolute value), and the smaller the p-value, the more sensitive the parameter. In this study we performed 1000 parameter set samples to investigate parameter sensitivity.

To differentiate between the SM1 and SM2 models, a regional parameterization approach was used in SM1 to further differentiate the 109 parameters in each of the 17 river basins separately (Fig. 1a). For example, the CN2 of forested areas in the upstream highlands were differentiated from those of downstream areas resulting in a better representation of spatial variability as compare to SM2, where the parameters were treated similarly all over the province. We again performed stepwise sensitivity analysis in the SM1, which resulted in a total of 1402 spatial parameters. Overall, more detailled differentiation of the spatial parameters in SM1, and a multi-gauge calibration scheme in this scenario model (e.g., 130 stations rather than six stations at the outlet of main river basins in SM1) allowed better representation of the hydro-climatic and spatial heterogeneity within each river basin. Similarly, the crop parameters were separately differentiated in SM1 and calibrated for each county, where crop yield data are available from Alberta Agricultural Financial Services Corporation (AFSC, Table S3).

In SUFI-2, parameter uncertainty is described by a multivariate uniform distribution in a parameter hypercube, while the output uncertainty is quantified by the 95% prediction uncertainty band (95PPU) calculated at the 2.5% and 97.5% levels of the cumulative distribution function of the output variables (Abbaspour et al., 2004, 2007). Latin hypercube sampling is used to draw independent parameter sets, which lead to the calculation of 95PPU for a given output variable. Parameter uncertainty here accounts for all sources of uncertainties, i.e., input uncertainty, structural uncertainty, as well as parameter uncertainty. The reason is that the calibration result, which is represented by the 95PPU, tries to capture "most" of the observed data. Observed data is the combination of all the inputs and processes in the system. Hence, if the model captures the observed data in the 95PPU, then all uncertainties are accounted for by the parameter ranges. It has to be mentioned that in the models where only a single variable is calibrated (e.g., streamflow) the estimated parameter uncertainties will not compensate adequately for the model structure uncertainty, when the model is used for prediction of conditions beyond the calibration base (e.g., actual ET) (Faramarzi et al., 2009; Refsgaard et al., 2007). Two statistics quantify the goodness of fit and model output uncertainty. These are the *p*-factor, which is the percentage of measured data being bracketed by the 95PPU, and *r*-factor, which is the average thickness of the 95PPU band (Abbaspour et al., 2004, 2007). The *p*-factor has the highest value of 1, while the lowest value for *r*-factor is zero. For flow, Abbaspour et al. (2007) suggest a practical value of 0.6-0.8 for the *p*-factor and a value around 1 for the *r*-factor. In this definition, (1-*p*-factor) can be thought of as model error, or measured points not accounted for by the model. For the comparison of the measured and simulated monthly streamflow, the following efficiency criteria (Φ_1) was calculated based on monthly streamflow data of hydrometric stations across each river basin (slightly modified Krause et al., 2005):

$$\Phi_1 = \begin{cases} |b|R^2 \text{ for } |b| \le 1 \\ |b|^{-1}R^2 \text{ for } |b| > 1 \end{cases} \tag{2}$$

where R^2 is coefficient of determination, and b is the slope of the regression line between measured and simulated streamflow. As R^2 only reflects the linearity of the two signals, including b guarantees that runoff under- or over-predictions are also reflected. A major advantage of this efficiency criterion is that it ranges from 0 to 1, which compared to Nash-Sutcliff Efficiency (*NSE*) coefficient with a range of $-\infty$ to 1, ensures that in a multi-site calibration the objective function is not governed by a single, or a few, badly simulated stations. It should also be mentioned that although bR^2 alone is used as the objective function, we also examined ten other efficiency criteria plus a visual inspection of the performance of each discharge station (these options are available in SWAT-CUP). Mathematically, in Eq. (2), as b becomes smaller than -1, the objective function value becomes larger than R^2 giving the impression of a better model performance. This, however, does not happen in practice as the discrepancy between observation and simulation would in this case be too large for that station to be considered for calibration. In such cases, the model must be re-examined as this would not be a calibration issue. In our work, we report the average R^2 and *NSE* as additional information to evaluate the model performance.

For each river basin with multiple measuring stations, the objective function (g) was expressed as:

$$g = \frac{1}{n}\sum_{i=1}^{n}\Phi_i \tag{3}$$

where n is the number of stations within each river basin. The objective function to calibrate crop yield was the Root Mean Squared Error (Eq. (4)), which was optimized initially before river discharges were calibrated.

$$RMSE = \frac{1}{n}\sqrt{\sum_{i=1}^{n}(Y_{o,i} - Y_{s,i})^2} \tag{4}$$

where n is the number of years for which the observed yields are calibrated in each county, Y_O is the observed yield, and Y_S is the simulated yield. The crop yield was simulated at the subbasin level and further aggregated to the county scale in order to compare with the AFSC reported yields.

As noted previously, the model was calibrated and validated for the periods 1993–2007 and 1986–1992, respectively.

2.3. Water use

We estimated the level of water use in 2014 for municipalities, oil and gas, commerce, industry, and others (e.g., water management projects (WMP) for water conservation objectives) to analyze monthly water supply/demand concerns in the province. According to ABENV (2007), the water use of non-agricultural sectors is almost uniform during the year, whereas agriculture (mainly irrigated crops) requires water only during the growing season. Therefore, we used the monthly simulated water consumption of wheat (dominant water intensive crop) from this study and the monthly water consumption data of the other irrigated crops from AAF and ABENV (2007). Livestock water use was calculated as a product of per capita livestock water consumption and the population of livestock for each river basin. Municipal water use was calculated as a product of per capita water use and the population of each river basin. Total oil and gas water use includes oil sands in situ and surface mining production, and the gas/petrochemical plants. The water use for in situ and mining production (*WUS*, m^3) was calculated as follow:

$$WUS = 0.159 \times (W/O) \times P \tag{5}$$

where *W/O* is the amount of water (in barrels) used to produce one barrel of oil; *P* is total amount of oil produced every year (barrels); and 0.159 is a factor to convert a Canadian barrel to m^3. The *W/O* ratio of each sub-sector was obtained from different sources (see Table S4). For the gas and petrochemical sector we used 20.6% of what is used in the petroleum sector (ABENV, 2007).

To account for the water demand of environment sector, we used the subbasin-based hydrological data of calibrated SM1 to calculate EFR on a monthly basis. We used the approach recommended by Tennant (1976), for which a 30%–50%, 20%–40%, 10%–30% renewable water availability must be allocated to maintain excellent, good, and moderately degraded levels of habitat quality, respectively. The ranges in Tennant approach represent the monthly variation of the EFR.

Table 1
Calibration performance in different river basins. The averaged NSE and R^2 are based on the best performing parameters obtained through optimizing the goal function (i.e., bR^2). The bold values present total number of parameters and average statistics in Alberta.

River basin	Nr. of parameters	Nr. of calibrated stations	Nr. of iterations to calibrate	*p*-factor	*r*-factor	Objective function 'g' pre-calib.	Objective function 'g' post-calib.	*NSE*g post-calib.	Nr. of stations with negative *NSE*	R^2 post-calib.
Athabasca	230	40	7	0.65	1.10	0.25	0.47	0.21	8	0.58
Battle	17	5	5	0.78	1.15	0.27	0.56	0.28	1	0.68
Beaver	34	3	4	0.63	1.51	0.13	0.39	0.23	1	0.56
Bow	124	11	5	0.40	0.75	0.27	0.46	−1.53	3	0.54
Hay	72	3	3	0.67	1.07	0.21	0.46	0.31	1	0.53
Milk	60	2	5	0.66	1.38	0.15	0.35	−0.04	1	0.44
North Sask.	158	13	4	0.55	1.35	0.34	0.41	−1.05	3	0.53
Oldman	200	16	6	0.54	0.67	0.26	0.39	0.15	4	0.50
Peace	151	22	5	0.66	0.87	0.34	0.44	0.31	5	0.57
South Sask.	35	1	3	0.48	0.75	0.52	0.69	0.57	0	0.76
Slave	30	1	3	0.88	0.58	0.42	0.79	0.81	0	0.85
Red Deer	189	13	5	0.64	1.35	0.28	0.34	0.12	4	0.40
Alberta	**1300**	**130**		**0.63**	**1.04**	**0.28**	**0.48**	**0.03**	**31**	**0.58**
Irrigation districts	40	10 counties	3	0.92	1.49	0.89	0.25 (RMSE)	-		-

It must be pointed out that water demand of non-irrigated sectors was available at the river basin scale. Therefore, we aggregated other water demand data (e.g., irrigated crops and environment) from county/sub-basin into the river basin scale to harmonize them for the analysis of water scarcity in later sections.

3. Results and discussion

3.1. Calibration, validation and uncertainty analysis

With the specifications provided for SM1 and SM2 models, we parallelized calibration of the models in a modern PC environment with 32 processors (CPUs) and within a Windows platform.

3.1.1. SM1 scenario model results

A multi-gauge and multi-objective calibration using crop yields and river discharges in SM1 ensured proper apportioning of precipitation and soil water into surface runoff, actual evapotranspiration, and groundwater recharge. This improved model performance as compared to pre-calibration model (Table 1, Fig. 2). Overall, 63% of the observed streamflow data were captured by the simulated 95PPU and the average *r*-factor was about 1.04 at the Alberta scale. While the average bR^2 of the 130 stations was 0.48, it varied from 0.11 to 0.89 for individual stations (Fig. 2). The negative average *NSE* in the Bow, North Saskatchewan, and Milk river basins was due to degraded *NSE* values in 3, 3, and 1 head-water stations, respectively (Table 1). Model performance of the pre-calibration step (Fig. 2a) was considerably improved after calibration (Fig. 2b). Except for the head-water stations in mountainous regions, most of the observed data (*p*-factor > 40%) were bracketed by relatively small 95PPU values (*r*-factor < 1.38) (Fig. 2c–d).

It is important to mention that before calibration of the model, we built different SWAT models using various climate data to determine sources of error resulting in poor performance of mountainous stations. Climate data were obtained from MS, Climate Research Unit (CRU), Natural Resource Canada (NRCan), and CFSR sources (Faramarzi et al., 2015). In this pre-calibration exercise we found that in snow dominated regions temperature was the most influential parameter to the hydrology. We found MS precipitation and the CFSR temperature data best represented the trend and fluctuations of streamflow simulation (Fig. 3a–e) prior to calibration. This model, was selected as our base model (e.g., SM1) for further sensitivity and calibration analysis and the results were further improved after calibration (Fig. 2b–d, and Fig. 3f). We also found that partial accounting of SWAT for glaciers was another source of error resulting in poor performance in head-water stations, especially during late summer and early fall. However, by adding the elevation band and a detailed parameterization of snow parameters as well as using the monthly glacial contribution to streamflow from Marshall (2014), which were spatially distributed using the percent coverage of the glaciers obtained from the GLIMS map (Fig. 1b), we significantly improved the snow/glacier melt simulation in SWAT.

Potholes and lakes in the south-eastern portion of the province posed another difficulty for accurate simulation of streamflow in our initial (default) model run (Fig. 4a). We were able to simulate most of the processes through incorporating the map of potholes and calibrating the related geo-spatial parameters (Table S5). The objective of our large-scale study was to assess the hydrologic effects of the potholes on downstream hydrology in south-eastern river basins. Our simulation at the subbasin level did not explicitly represent the dynamic relationship between potholes within each subbasin, but rather represented aggregated effects of the potholes in each subbasin on hydrological behavior. We therefore calibrated parameters POT_FR, POT_VOLX, POT_VOL, SOL_K, SOL_AWC, GW_REVAP, and GWQMN (see Table S5) to simulate the hydrological water balance of the pothole-dominated subbasins. Overall, simulation of the potholes improved simulation of the processes

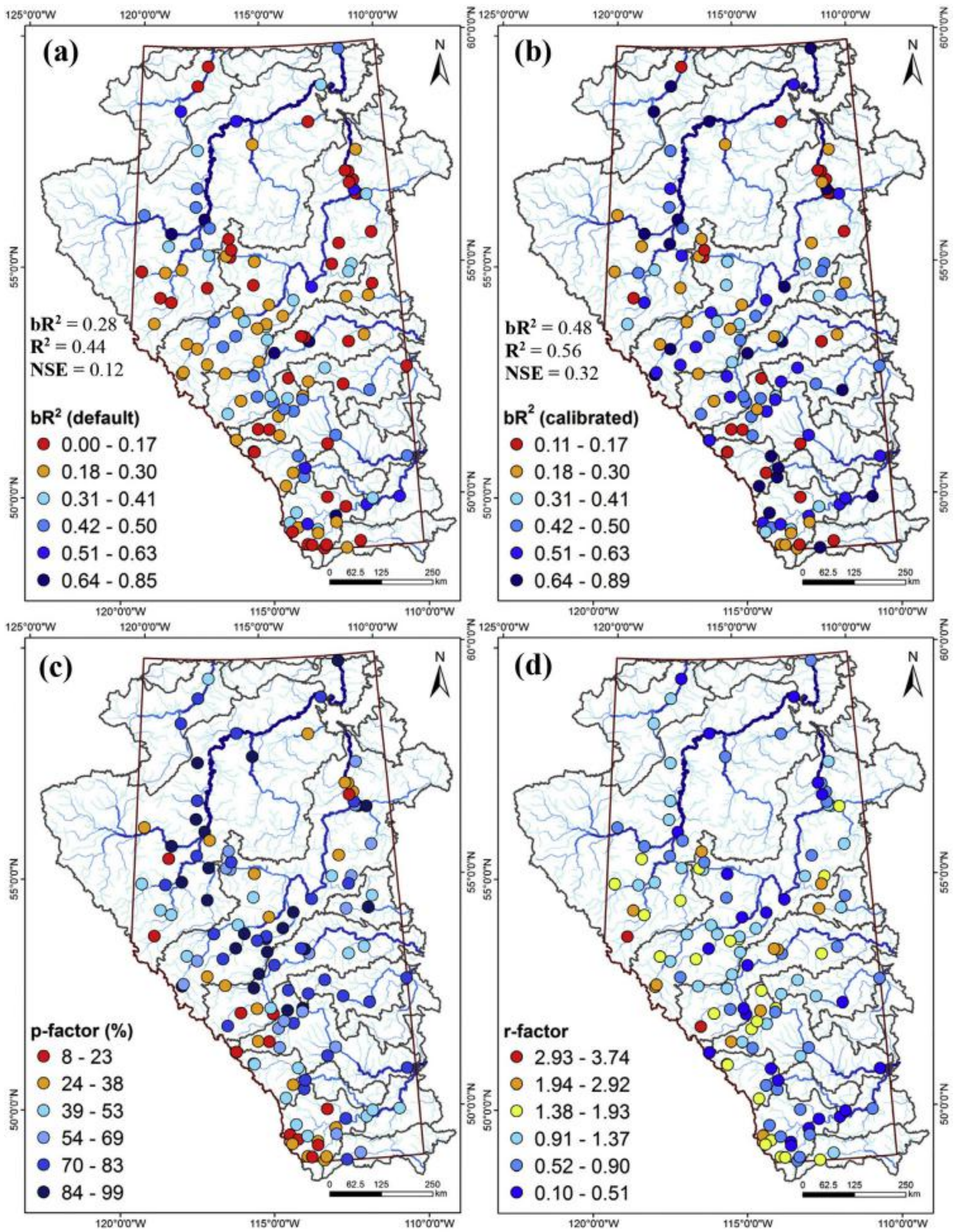

Fig. 2. Model performance of pre-calibration (a), and post-calibration (b) at 130 hydrometric stations; and calibration-uncertainty performances including the *p*-factor (c) and the *r*-factor (d). Provincial statistics (bR^2, R^2, and *NSE*) are provided in Fig. 2a-b legend for the evaluation of model improvement.

apportioning precipitation into surface runoff, evaporation, and infiltration. The net result was a considerable improvement in the simulation of related streamflows (Fig. 4a–b).

Natural lakes and man-made reservoirs are important features that introduce heterogeneity into land-surface parameterization and related hydrological processes. We therefore, incorporated and simulated the operation of 14 regulated dams (Fig. 1) and one natural lake in the Athabasca River Basin (i.e., Lesser Slave Lake), that have the largest influence on downstream flows. We found that correct simulation of dam/lake outflows is strongly connected to a proper simulation of the upstream catchments feeding these reservoirs.

In general, the calibration and validation performances were satisfactory for most of the river basins and stations (Fig. S2). We predicted uncertainty for different stations to map the errors related to climate, geo-spatial parameters, potholes, dams, glaciers, and (fossil) groundwater contribution where the data are not adequately represented and the process are simplified in the model (Fig. 4c,d). More uncertainty in the predictions partially implies poorer data quality and quantity.

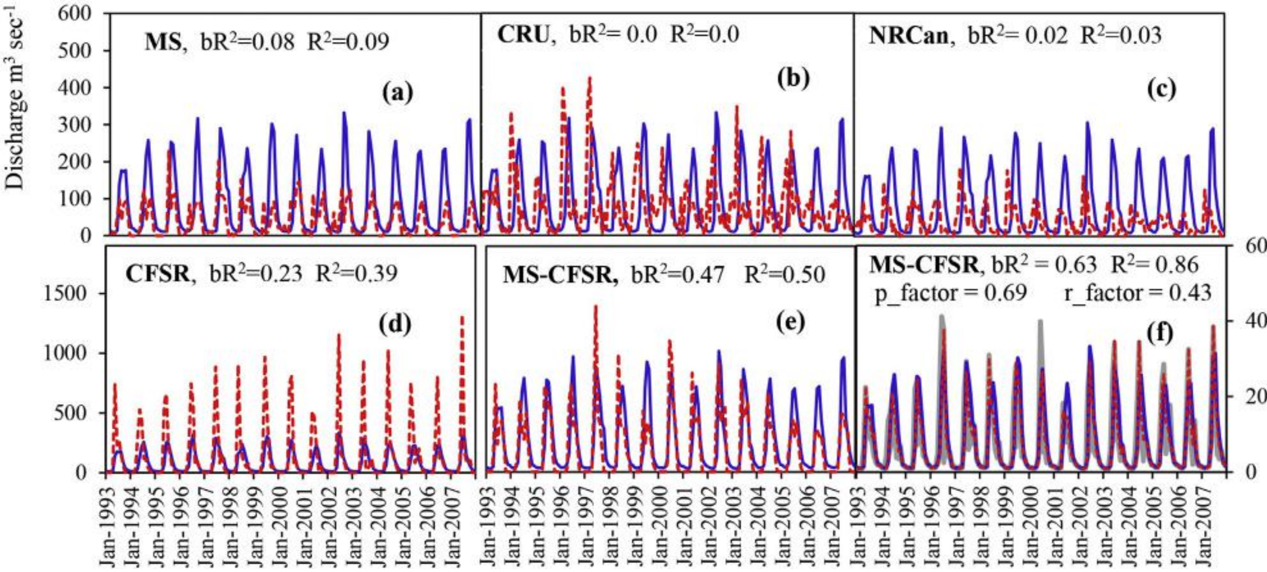

Fig. 3. Observed (blue) and simulated (red) streamflow at Athabasca Near Jasper station (drainage area of 386 km^2), located at one of the head-water tributaries of Athabasca River Basin and influenced by snow melt and glacier runoff, using different climate datasets. The grey band (f) is the 95% prediction uncertainty.

Table 2
Comparison of calibration performances of the two model scenarios in six main outlets. The bold values present average statistics of the study area.

River basin	*p*-factor		*r*-factor		*bR*^{2}	
	SM1	SM2	SM1	SM2	SM1	SM2
Peace-Slave	0.95	0.80	1.32	1.16	0.80	0.73
Hay	0.72	0.88	1.40	0.58	0.66	0.79
Athabasca	0.94	0.80	1.46	0.57	0.73	0.66
North Saskatchewan	0.74	0.63	1.10	0.71	0.58	0.70
Red Deer	0.95	0.80	3.79	1.37	0.58	0.63
South Saskatchewan	0.79	0.48	1.75	0.75	0.67	0.69
Average	**0.85**	**0.73**	**1.80**	**0.86**	**0.67**	**0.70**

For example, the lack of good quality climate data for northern remote areas adds more prediction uncertainty (e.g., Fig. 4d, larger r-factor).

Irrigated areas in southern watersheds posed another challenge in our large scale hydrological model. As already mentioned, our objective was to achieve an accurate representation of the soil water balance in irrigated lands, and therefore the blue and green water components (Falkenmark and Rockstrom, 2006) in these regions. Calibration and validation of the model against irrigated wheat yield (Fig. 4e,f) ensured a proper apportioning of the soil water to crop ET and groundwater recharge. In the SWAT model, simulation of crop yield and crop ET are closely related to nutrients, climate, and soil moisture, among other factors. As we only calibrated crop yield, we compared the simulated crop ET against available data from AAF to increase confidence on simulated crop ET. As shown in Fig. 4g,h, most of the AAF data are bracketed within our simulated 95PPU. Similar to other output variables, the prediction uncertainty in irrigated wheat yield ensured an adequate representation of the errors related to model simplification, geo-spatial parameters, and other data affecting crop growth (Fig. 4e,f). It is imperative to note the importance of uncertainty analysis in a distributed model, as it highlights the areas of data gaps and model process limitations. Our findings clearly provide direction for future data collection and model development attempts.

3.1.2. SM2 scenario model results

As we mentioned previously, we built SM2 to study the effect of improper simplification of large-scale hydrological models (similar to that of high grid-resolution global models) on process representation at the subbasin spatial scale and monthly level. Similar to SM1, the SM2 model performed well in simulation of streamflow patterns in the main outlets (Table 2). With an average bR^2 value of 0.67–0.70, the *p*-factor and *r*-factor were satisfactory for all six stations under the two scenarios. However, the corresponding hydrological processes and water balance components in upstream catchments were significantly different under the two scenarios (see the results in the later section).

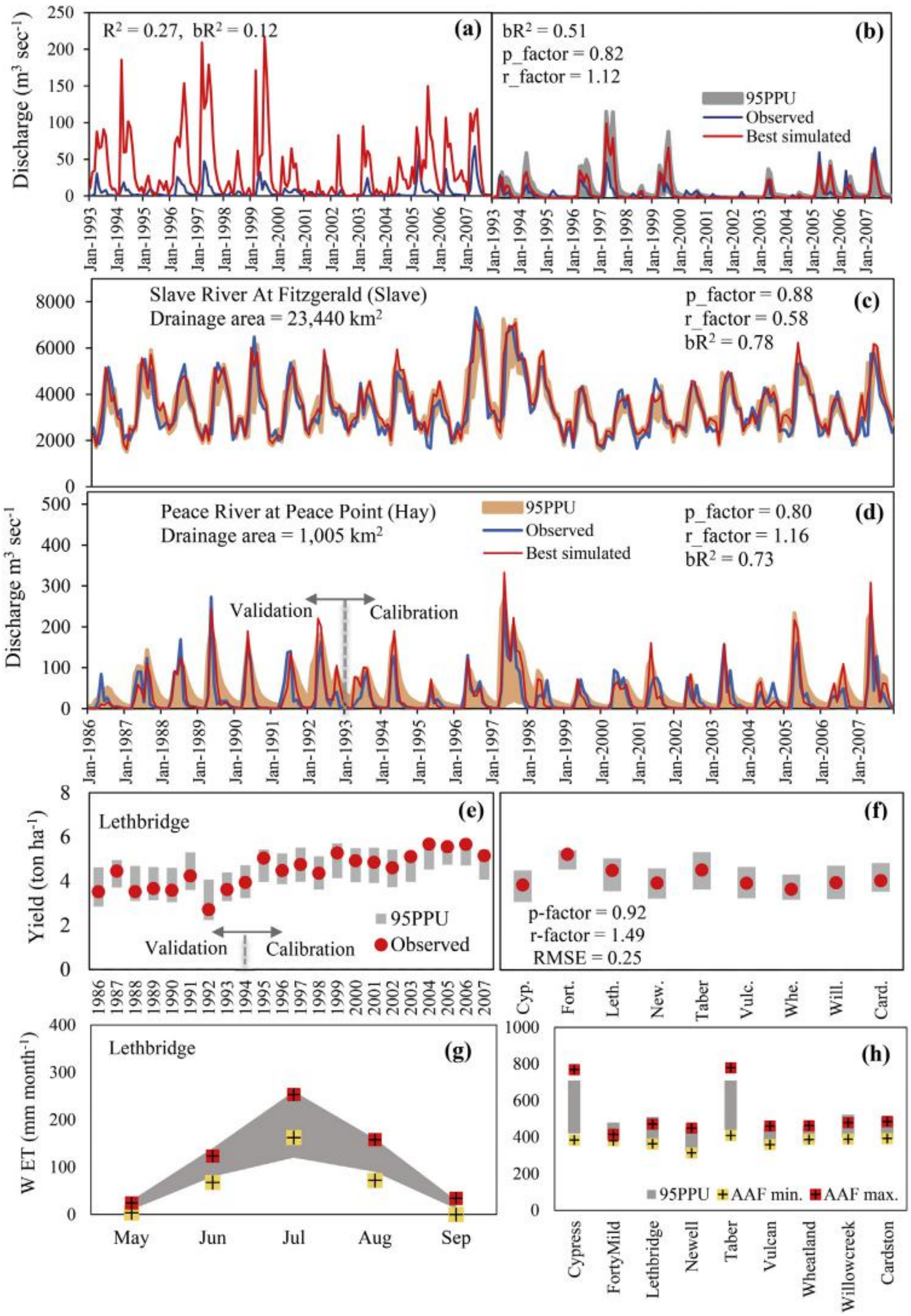

Fig. 4. Calibration, validation and uncertainty results: observed and simulated streamflow for a selected station in Battle River (drainage area of 2598 km^2) without pothole (a) and with pothole (b); observed and simulated discharges for two selected hydrometric stations in different river basins (c,d). The best simulation (red line) maximized the objective function and was used to narrow the uncertainty band in subsequent iterations (more examples are provided in Supplementary Fig. S2); observed and simulated (95PPU) annual wheat yield of Lethbridge county (e) and the average annual yields of different provinces (f); and the observed (AAF) and simulated (95PPU) of the monthly wheat ET (WET) in Lethbridge (g); and total ET in different counties (h) over the years 1986–2007.

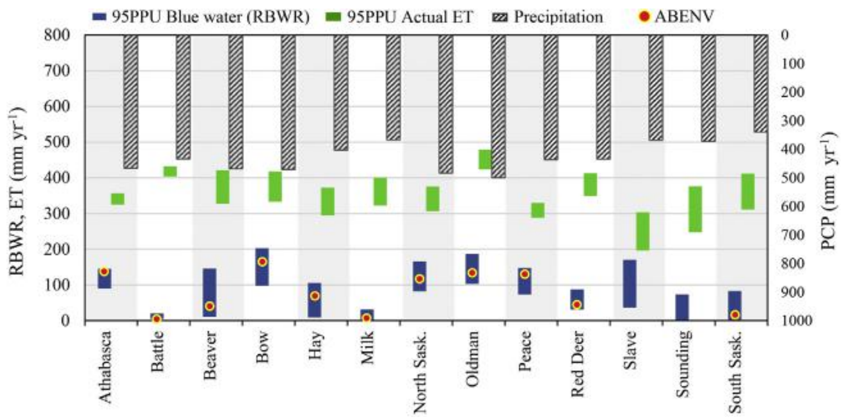

Fig. 5. Modelled average (1986–2007) annual renewable blue water resource (RBWR), actual evapotranspiration (ET, green water flow) expressed as 95% prediction uncertainty, and precipitation (PCP) for different river basins in Alberta. The ABENV reported blue water data are shown for comparison with the model outputs.

Table 3
Average precipitation and the 95PPU ranges for the water resource components in the Alberta's river basins. PCP: precipitation; Blue: renewable blue water; ET: actual evapotranspiration; SW: soil water; GW: groundwater recharge; DP: deep aquifer recharge; BS: base flow. Simulated variables are in km^3.

River basin	PCP	Blue	ET	SW	GW	DP	BS
Athabasca	71.06	13.67–24.19	49.67–54.51	20.57–28.33	6.18–12.58	0.28–0.75	4.41–9.71
Battle	11.58	0.13–0.54	10.76–11.54	1.36–1.62	0.18–0.44	0.01–0.03	0.02–0.37
Beaver	7.52	0.18–2.35	5.26–6.77	1.34–3.38	0.10–1.86	0.00–0.13	0.02–1.39
Bow	12.29	2.56–5.29	8.70–10.91	0.95–1.80	0.10–1.50	0.00–0.10	0.00–0.10
Buffalo	4.26	0.98–1.48	2.31–3.23	0.21–0.92	0.01–0.11	0.00–0.00	0.00–0.00
Great Slave Lake	0.48	0.21–0.35	0.11–0.19	0.00–0.00	0.00–0.00	0.00–0.00	0.00–0.00
Hay	18.90	0.41–4.94	13.82–17.50	7.60–14.06	0.28–4.10	0.01–0.28	0.02–3.04
Lake Athabasca	4.07	0.89–1.24	1.96–2.96	0.33–0.63	0.38–0.68	0.02–0.05	0.22–0.31
Liard	2.29	0.38–0.89	1.08–1.67	0.54–0.82	0.00–0.00	0.00–0.00	0.00–0.00
Milk	7.02	0.03–0.60	6.16–7.66	0.62–1.17	0.01–0.43	0.00–0.03	0.00–0.29
North Sask.	28.58	4.89–9.84	18.19–22.29	3.31–6.23	0.69–4.07	0.03–0.26	0.17–2.77
Oldman	13.48	2.79–5.05	11.46–12.96	1.37–1.99	0.41–1.85	0.02–0.12	0.02–0.12
Peace	105.74	17.83–36.05	70.46–80.77	28.36–42.09	5.79–19.46	0.24–1.22	2.97–13.87
Red Deer	20.32	1.45–4.11	16.39–19.37	2.13–3.28	0.45–1.73	0.02–0.11	0.02–0.11
Slave	4.61	0.46–2.13	2.46–3.81	0.36–1.45	0.06–0.81	0.00–0.06	0.02–0.63
Sounding	6.05	0.03–1.19	4.04–6.13	0.23–0.82	0.04–0.82	0.00–0.05	0.00–0.52
South Sask.	6.20	0.04–1.52	5.68–7.53	0.23–0.72	0.01–0.58	0.00–0.04	0.00–0.04

3.2. Quantification of water resources at regional and subbasin levels

3.2.1. SM1 scenario model results

Monthly water yields were simulated for all 2255 subbasins. The water yield (WYLD) in SWAT is the amount of water leaving a hydrologic response unit (HRU) and entering the main channel during the simulated time-step. We used model outputs to calculate blue water (sum of water yield and deep aquifer recharge), green water flow (actual evapotranspiration), and green water storage (soil moisture) as defined by Falkenmark and Rockstrom (2006). We aggregated the simulated blue water of subbasins to calculate that of each river basin at a monthly time-step. We found that the estimated blue water of ABENV (2008), which is based on historical records, is bracketed within our uncertainty predictions (Fig. 5). This provides a verification of our calibrated model results. In general, for most of the river basins green water flow has a larger share of available water than blue water component (Fig. 5, Table 3). A large ET in northern river basins is due to the evapotranspiration occurring in mixed wood, broadleaf, and coniferous forests and associated wetlands. In southern watersheds, ET is due to the irrigated areas where crop water consumption dominates the other water components.

For inter-comparison of freshwater components we used the median of 500 simulations (M95PPU) of the calibrated model, and created the maps shown in Fig. 6 for the study period. It is important to note that the reported uncertainty depicts temporal variability in climate as well as the model uncertainty resulting from model assumptions and simplifications, parameter uncertainty, and errors in model input data including climate, soil, landuse, etc. What is most striking is the large spatial variation in hydrological variables across the province. Overall, the western mountainous regions receive the largest amount of precipitation (Fig. 6a), while southern and eastern watersheds receive a smaller amount and experience higher temperatures (Fig. 6b,c). The spatial pattern of snowfall and snowmelt (Fig. 6d,e), which were simulated based on temperature, accumulation or shrinkage of snowpack, and sublimation, agreed well with the precipitation data.

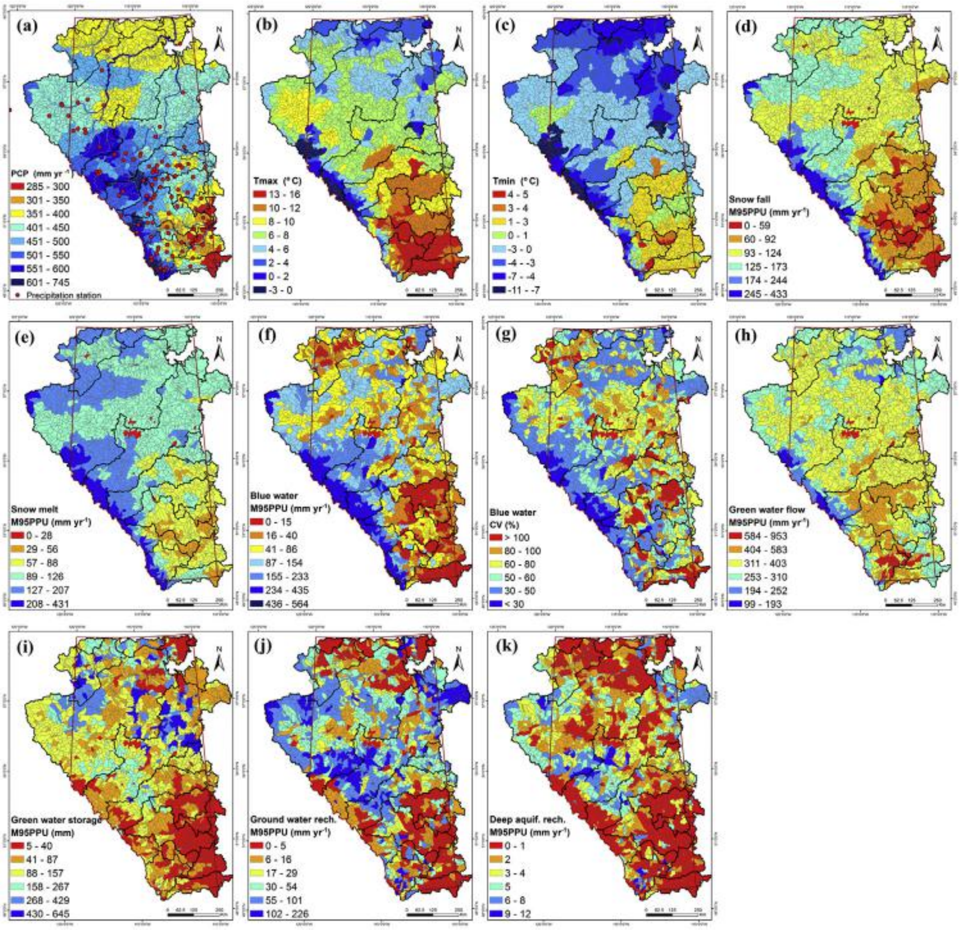

Fig. 6. SWAT simulated precipitation (a), maximum and minimum temperature (b,c), snow fall (d), snow melt (e), and blue water (f), actual evapotranspiration (h), soil moisture (i), groundwater recharge (j), and renewable groundwater (k) averaged based on monthly predictions of the M95PPU (i.e., median of 500 simulations) during 1986–2007 period.

It is noteworthy that the spatial variation of the SWAT simulated precipitation, temperature, and snowfall is similar to the ABENV (2007) reported data. This provides a stronger confidence to our simulation results, especially for the mountainous regions where snowfall is significant but does not immediately contribute to streamflow. Improved temperature and precipitation input through combination of multiple datasets, as well as snow related parameters in highland subbasins (e.g., Fig. 3), resulted in a more accurate representation of the snow hydrology in these regions. Of the 500–700 mm precipitation (Fig. 6a) in the western high altitudes, about 150–560 mm is renewable blue water resources (RBWR) (Fig. 6f). This water supplies most of the downstream subbasins in the south where the internal renewable blue water is meager and agriculture is intensively practiced. The annual coefficient of variation (CV) (Fig. 6g), represents the reliability of water resources and gives practical insights for water resource managers and decision makers concerned with long-term planning for various economic sectors. Larger green water flow occurs in agricultural lands and irrigated districts (Fig. 6h). This pattern corresponds well with the green water storage (Fig. 6i) where it drops to its minimum depth in the agricultural lands. This implies that the high evaporative demand of crops, due to higher temperatures, must be compensated by soil moisture and eventually irrigation. Overall, the green water component showed less spatial and temporal variation (Fig. S3) compared to the blue water component. Schuol et al. (2008) attributed this fact to a limited storage capacity of the soil.

The groundwater recharge (GWRCH) in SWAT is defined as the amount of water entering shallow (GW) and deep (DP) aquifers. SWAT allows this water to be further discharged into the rivers as return flow or moved to the root zone through capillary rise (i.e., revaporation) during times of high groundwater levels and large evaporative demands on a daily basis. The high GWRCH in central and northern watersheds (Fig. 6j) largely contributes to streamflow (i.e., base flow), soil evaporation, and plant water uptake. Therefore, only small amounts remain in shallow aquifers and will eventually end up in deeper aquifers allowing the formation of a more sustainable water resource (Fig. 6k). This renewable groundwater has quite a meager contribution to blue water resources as a whole (Fig. 6f) but may, if not exploited, represent a resource in the future.

It should be noted that groundwater is only calibrated indirectly in this study, as there were no groundwater recharge measurements at this level of detail for the province. However, to increase the confidence in model results we compared

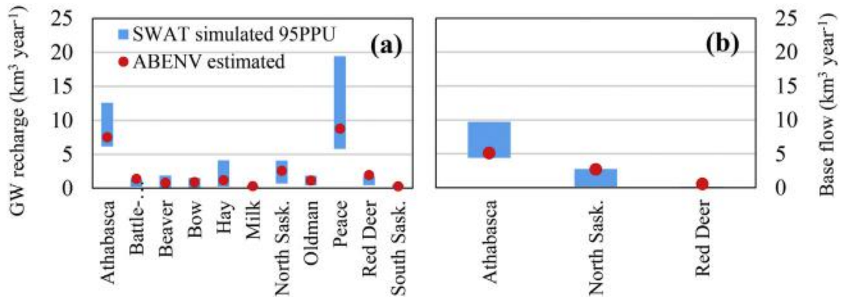

Fig. 7. Comparison of simulated and ABENV reported groundwater recharge (a), and base flow (b).

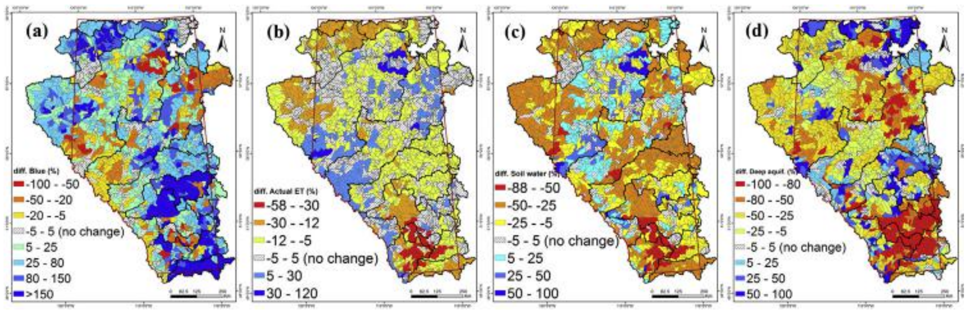

Fig. 8. The anomaly map of water balance averages: blue water (a), green water flow (actual ET) (b), green water storage (soil water) (c), deep aquifer recharge (d). The% differences are calculated based on the averages of data period 1986–2007 of SM2 from the SM1 simulation results as: [(SM2-SM1)/SM1] × 100.

the simulated regional GWRCH and the base flow with estimates made by ABENV (2008). We found that the estimated groundwater recharges made by ABENV are bracketed within our simulated results for most of the major river basins (Fig. 7). Overall, incorporation of the major hydrological features (e.g., a proper climate representation, glaciers, potholes, regulated dams/reservoirs, and irrigated agriculture) in the model, and providing an adequate calibration and validation of the soil related processes, resulted in a reliable groundwater recharge estimation.

3.2.2. SM2 scenario model results

Calibration of the SM2 model output only in the outlets of the six major river basins, a global parameterization scheme rather than regionally detailed representation, as well as the lack of process simulation of irrigated agriculture caused over- and under-estimation of the subbasin based water components throughout the watersheds. We show anomaly maps of the blue and green water components that were simulated using the SM1 and SM2 models (Fig. 8). The positive values show the percent over-estimation of the SM2 relative to SM1, while negative numbers show under-estimated values. Generally, in subbasins where SM2 over-estimated the blue water (e.g., southern half of the province and the north eastern subbasins), the green water components (e.g., actual ET and soil water storage) were under-estimated. Similar patterns are observed within the river basins. For example, three segments of change patterns are observed throughout the Athabasca River basin. The first segment in head-water subbasins show an under-estimation of blue water and over-estimation of green water components, while the second segment in the middle part of the river basin shows an opposite pattern with over-estimation of blue water and under-estimation of green water, followed by a different pattern in the downstream subbasins. The observed anomalies in these figures originate from an inadequate parameterization and calibration scheme in SM2. As mentioned before, in SM2, parameters were not regionalized based on land use and soil types. For example, the SCS curve number, CN2, of forested areas of upstream highlands were treated the same as those of downstream lowlands. In addition, they were not differentiated between river basins resulting in a loss of spatial variability in the model. This over-estimation in some subbasins and under-estimation in others caused the prediction errors to be completely offset throughout the river basin, and a similarly good calibration performance obtained only at the outlets (Table 2). Our results underscore the importance of building a locally representative model through a better parameterization scheme, and utilizing detailed local information (e.g., irrigated wheat) in water supply models. In addition, the results underline that a multi-gauge calibration, rather than only for main outlets, is key for an accurate accounting of water supply components. High resolution global models lack this level of resolution.

3.3. Implications of model results for water supply-demand concerns, regional economic activities, and global food security

Alberta has an export-oriented economy with the province's GDP strongly connected to water. While, agriculture consumes 60–70% of Alberta's water (ABENV, 2007), it only accounts for 1.5% of the provincial GDP (AARD- Alberta Agriculture

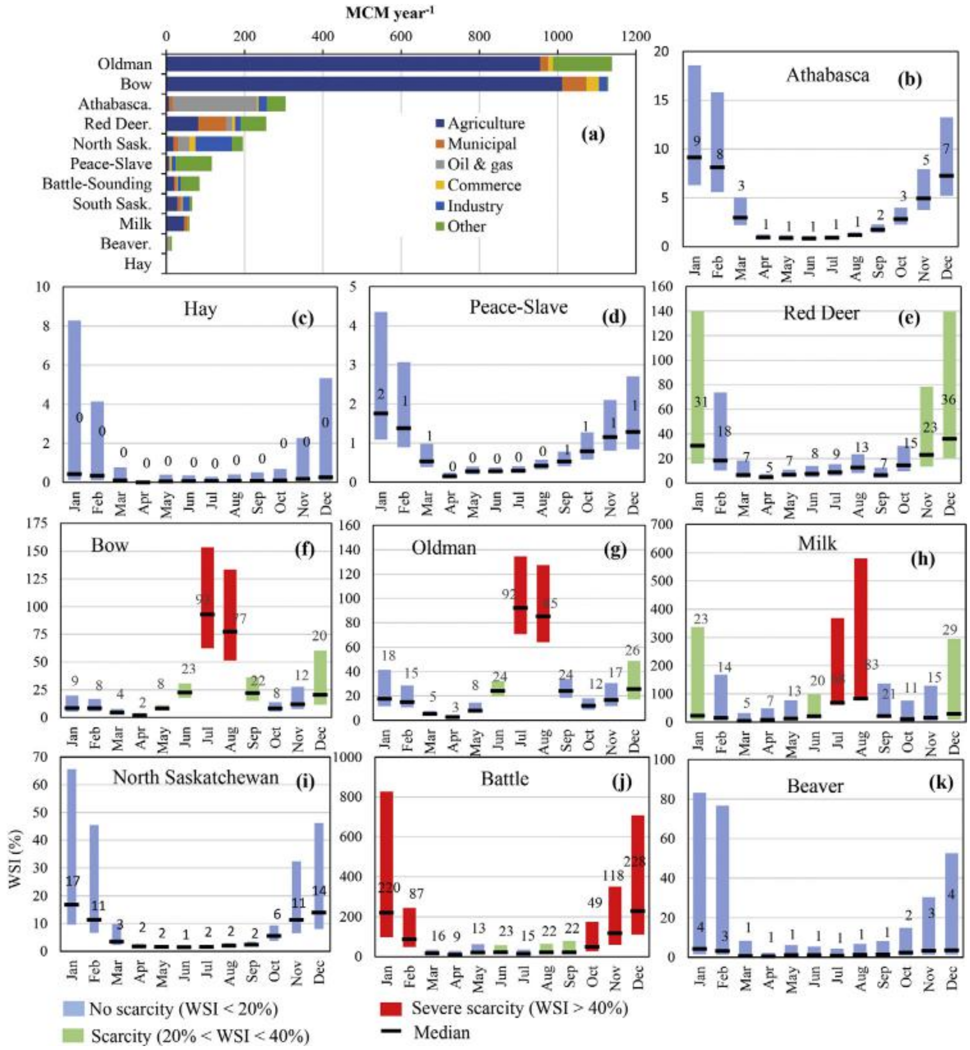

Fig. 9. Estimated water use of different sectors (a), and computed monthly water scarcity indicators (b–k) for different river basins. The WSI calculated as the ratio of water consumption to simulated renewable blue water resources (RBWR). The range is related to the use of L95PPU-RBWR and U95PPU-RBWR in the ratio. The colors, depicting severity of the scarcity, are specified based on the median of simulated RBWR.

Rural Development, 2010). Conversely, the energy sector, which supports 23.4% of the GDP (GOA, 2015), uses less than 3% of the available water. This disparity in the water-food-energy nexus creates strains between economic prosperity through oil and gas development, and has socio-political implications for the agricultural sector. Moreover, the province, like many jurisdictions around the world, is increasingly experiencing pressures on water resources due to population growth, industrial development, and climate change induced spatial and temporal variability. Using the modeled water supply data of SM1 and estimated water demand of various sectors (Fig. 9a) we calculated a water scarcity index (WSI) using the widely used indicators defined by Alcamo et al. (2007), Raskin et al. (1997), and Rijsberman (2006) (Fig. 9b–k). The 95PPU of RBWR resulted in a range of uncertainty predictions in the WSI. As stated before, the range of uncertainty reported here includes temporal year-to-year variation in climate as well as uncertainty due to model, input, and parameters. The severity of water scarcity (different colors) in each month is based on the median of simulated RBWR. Using only the lower band 95PPU of RBWR would increase severity of the scarcity in each month, hence producing an erroneous picture of the reality. We found that the severe water scarcity in most of the spring and summer months was mainly due to irrigation practices in southern watersheds (i.e., Milk, Oldman, Bow). Conversely, in winter months, water scarcity was mostly due to water demand of WMP, municipal, and other industries (e.g., Battle River basin; See Fig. S4). This underscores that water demand in water-deficit months are supplied from fossil groundwater exploitation or through storage during water-surplus months and allocation in water-deficit months. It must be pointed out that, in our calculations, we did not consider the EFR and apportionment requirements of the downstream provinces. Further, we used our subbasin-based simulated water supply data, and accounted for the EFR using Tennant method for the moderate, good, and excellent habitat levels in main river basins. The resulting water scarcity levels showed an increase of about 11% to 100% with the maximum amount of 174%

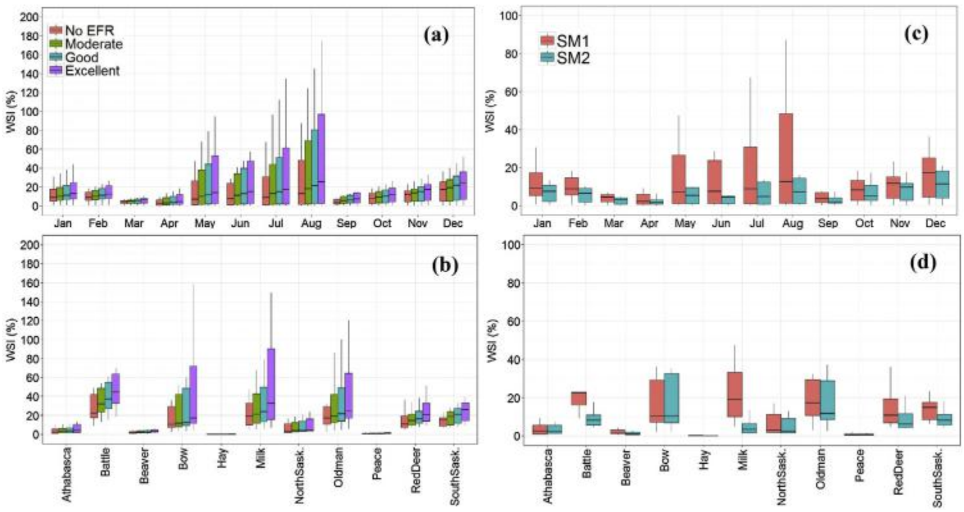

Fig. 10. Comparison of water scarcity indicator computed under various scenarios: The SM1 water supply results, the sector based water use data, and the EFR were used to maintain moderate, good, and excellent habitat quality at monthly (a), and river basin (b) scales. Comparison of WSI using SM1 and SM2 water supply data and sector based water use data, without consideration of EFR, at monthly (c), and river basin (d) scales. Box plots were created using the long term average M95PPU of the monthly WSI of different river basins.

occurring in August under the excellent habitat level at the provincial scale (Fig. 10a). However, the water scarcity indicator under various habitat levels varied across river basins (Fig. 10b). Under the excellent habitat level, where larger amounts of water are allocated to the environment, the Hay (with WSI of 0.6), Peace (with WSI of 2.5), Beaver (with WSI of 6.1), and Athabasca (with WSI of 13.1) river basins remained far below the 20% threshold level for the water scarcity. However, the severity of water scarcity increased in Oldman (from 87 to 174), Bow (from 79 to 158), Milk (from 74 to 149), Battle (from 48 to 69), and Red Deer (from 36 to 52) river basins, respectively, under the excellent habitat level. It is worth mentioning that requirement of 'one-half' of the annual natural river flow to the downstream provinces, and the release of 42.5 $m^3 s^{-1}$ during the minimum flow from Alberta to Saskatchewan will worsen the situation in southern river basins. Moreover, we aggregated subbasin-based data of SM1 and SM2 models to the river basin scale and investigated the effects of these two similarly good-performing models on WSI. We found that WSI was under-estimated in SM2 compared to SM1 (Fig. 10c). In addition, the range of WSI values in SM2 (e.g., the length of the box plots; Fig. 10c) was consistently smaller in all months compared to SM1, which was more evident during May to August. This implies a substantial under-estimation of WSI during spring and summer months. However, this under-estimation was different across river basins (Fig. 10d). The Battle, Milk, and Oldman river basins were exposed to the greatest under-estimation of about 65%, 84%, and 35%, respectively, compared to the SM1. Other river basins were either over-estimated (e.g., Bow) or slightly under-estimated. It has to be pointed out that although the watershed scale results showed a general under-estimation in the SM2 scenario, a finer scale estimation of WSI (e.g., subbasin) will result in a different pattern of over- or under-estimation within each river basin. Additionally, we used the county-based population data of the year 2011 from Statistics Canada (a total of 80 counties in the province), to account for the number of people facing water scarcity under different scenarios (Fig. 11). The results of SM1 showed that approximately 3.4 and 1.7 million people in Alberta live under condition of water scarcity (WS) at least one month and three months per year, respectively. The results showed that 3.2 and 0.22 million people experience severe water scarcity (SWS) at least one month and three months per year, respectively. However the SM2 simulated results showed less number of people experience both levels of water scarcity for at least one and three months of the year (Fig. 11, Table S6). Consideration of EFR to maintain river habitat at excellent, good, and moedrately degraded levels showed larger number of people under condition of WS and SWS compared to SM1 where no EFR was considered (Fig. 11, Table S6). This implies the importance of EFR to prevent under-estimation of WSI at high spatial and temporal resolution, where decisions are made and management practices take place.

It is worth mentioning that, while agriculture is the largest water consumer with the least economic revenue per volume of water used or consumed, any decision to reduce agricultural production to invest in more profitable industries is likely to affect national and global food security (see Fig. S1). To avoid restricting water supply to the agricultural sector, alternative options are suggested through increasing agricultural outputs per unit of water consumed (more crop per drop) (Faramarzi et al., 2010b; Molden et al., 2003), expansion and management of green agriculture (Falkenmark and Rockstrom, 2006; Lambin et al., 2013), improving the yield gaps (Schierhorn et al., 2014), and demand management (Adamowicz et al., 2010). Our analysis establishes a sound base to assess these alternatives in future research phases where the dynamic interactions of the water-food-energy nexus will be examined.

As part of the blue water assessment, groundwater (GW) scarcity is now becoming the subject of many research studies. The GW sustainability, defined as the balance of withdrawals and replenishment over time (Alley, 2006), has been inves-

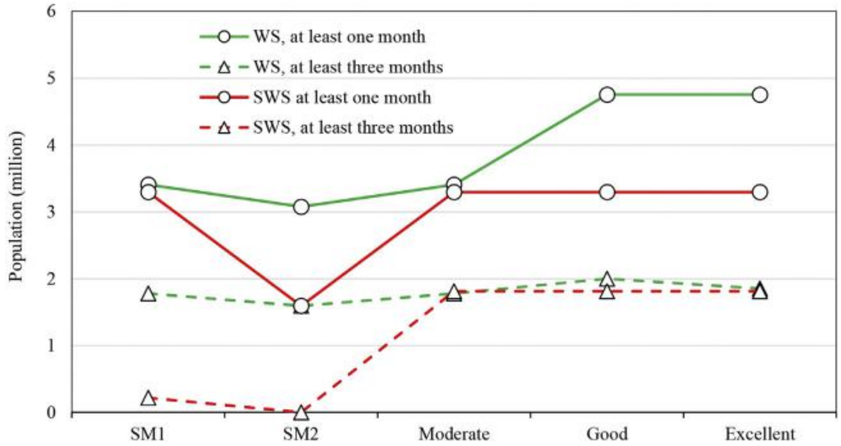

Fig. 11. Comparison of the estimated population size exposed to different levels of water scarcity under various scenario models. WS: Water Scarcity; SWS: Severe Water Scarcity.

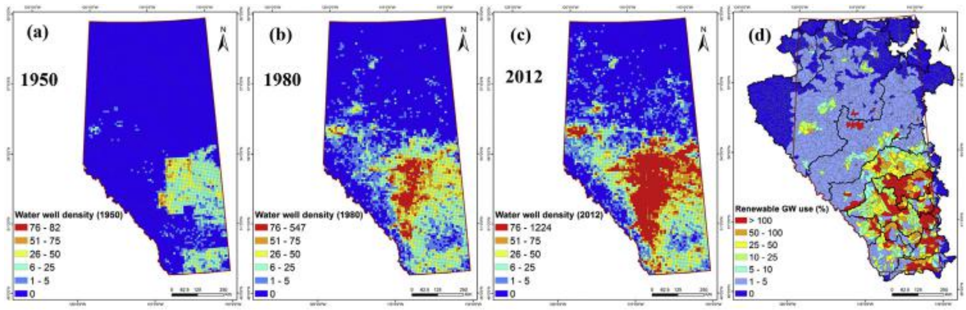

Fig. 12. Water well density of the years 1950 (a), 1980 (b), and 2012 (c) in Alberta at township grids (~92 km^2). Percentage of the GW use of the year 2012 compared to the long term average M95PPU of the simulated renewable GW recharge (d).

tigated under different assumptions and data resolution on withdrawal and availability. Recent advancements in satellite technology by NASA has allowed better representation of groundwater stresses at the global scale, as more accurate data on renewable and nonrenewable withdrawals are compiled (Beek et al., 2011; Doll, 2009; Richey et al., 2015; Wada et al., 2011). In Alberta, GW use varies by sector and location and has been intensified since 1950 (see Fig. 12a–c). Industry (oil and gas), agriculture, and municipalities are the largest consumers of GW accounting for 41%, 23%, and 19% of the total groundwater use, respectively. We used the grid-based water well density data for the year 2012, and GW use data provided by ABENV (2007); and aggregated them to the subbasin level. Groundwater use was calculated by means of gridded unlicensed water well density and licensed groundwater wells. Unlicensed well data were obtained from the Alberta Water Well Inventory Database (see, Table S4), and the active groundwater diversion licenses in the province were provided by AEP. Unlicensed groundwater use was estimated by assigning one household to each documented water well with AEP, assuming 2.6 people per household using an average annual volume of 76 m^3 per person. Daily water usage was estimated using the reported average for Albertans of 209 liters per person per day as cited by Environment Canada (see Table S4). We considered volumes of groundwater use within each density cell and then aggregated to subbasin level. Further, we divided the water use data by our simulated subbasin level recharge data (renewable GWRCH, Fig. 6k) to address the GW stress at the subbasin level (Fig. 12d). We found GW stress in most of the southern subbasins that are already exposed to some degree of blue water scarcity. It must be noted that GW systems are not static in actual conditions, and respond to the balance between supply (recharge), demand (use), and connectivity between aquifers (Best and Lowry, 2014). While our simulated recharge is based on a robust calibration-validation analysis, and most of surface hydrological features and dynamic-physical processes have been addressed in the 1–2 m soil layer; GW flow has not been explicitly simulated and sub-basin based GW water use has not been systematically involved in GW simulation process. Therefore, our results do not account for the GW connectivity that may alleviate scarcity in the short-term. In addition, we have simulated water consumption of irrigated wheat as the dominant and representative crop in our hydrological model. Meanwhile, water consumption of other crops and other sectors (e.g., municipal, industry, etc.) have not been systematically employed in the model to account for the temporal fluctuations. Overall, our results are an indication of the potential stress conditions in different subbasins where more detailed analysis and modeling efforts are required for representation of dynamic groundwater and surface water processes, as well as potential water scarcity.

4. Conclusions

This study contributes to the assessment of water scarcity and freshwater resources in a jurisdiction with heterogeneous watersheds, where conflicts over water resources have arisen between various sectors. Using the province of Alberta as a case study, we addressed cumulative effects of the natural features (e.g., climate, glaciers, potholes, soil, vegetation) and the anthropogenic factors (e.g., regulation through dams, irrigated agriculture, industrial development) on catchment hydrological responses and the dynamics of blue and green water resources at the subbasin level, where water scarcity is quantified. We addressed the most important challenges with respect to hydrological model building, calibration, and uncertainty assessment in various river basins of Alberta where hydro-climatic, data quantity and quality, and management conditions are diverse; and the dynamical processes are not simulated explicitly in the model (e.g., glacier, GW base flow, and pothole effects on drainage). We found that temperature was the most sensitive factor altering hydrological processes in the western snow-dominated areas. Nevertheless, geo-spatial parameters were also sensitive to streamflow simulation in lowland regions of these river basins. Glacier runoff contribution and snow parameters had a large influence on streamflow simulations of the head-water areas in most of the river basins. The anthropogenic changes on river systems (e.g., regulation through dams) as well as climate and other factors had significant impacts on the flow regime of southern river basins. Many small to large lakes and potholes of the eastern watersheds in southern part of the province had a considerable impact on the hydrological simulations. We improved our over-estimated streamflow simulation through inclusion of potholes and calibration of related processes in the model. Overall, we found that disregarding major hydrological features resulted in inadequate calibration and validation of the model. Without adequate representation of the processes, parameters would erroneously be fitted resulting in misleading assessment of water scarcity and overall water resources. We also quantified uncertainty in predicted water supply components and highlighted the importance of uncertainty analysis in a distributed model, as it underscores the areas of data gaps and model process limitations.

We applied the calibrated-validated model to simulate freshwater availability. Using the modeled water supply and estimated water demand of various sectors, we computed monthly blue water scarcity of different river basins. We found that severe water scarcity in most of the summer months it was mainly due to irrigation practices in southern watersheds, whereas in winter months was mostly due to water demand of WMP, oil and gas, and other industries. In addition, we found that water demand data are critical in the analysis of water scarcity. The use of sector-based detailed and local data rather than national or regional average statistics, as well as assessment of EFR, results in a more accurate accounting of water scarcity.

Finally, we used the simulated renewable recharge data to account for the share of groundwater use in the province. We found higher use of the groundwater in southern subbasins resulting in increased stress based on the assessment completed. Although the groundwater flow and connectivity, and hence the dynamic response of the groundwater to withdrawals and use, have not been simulated in our large scale SWAT study, we highlighted subbasins where more detailed analysis on the dynamic relationship between surface water, groundwater recharge and flow, and groundwater use would be required.

Overall, our analyses and associated results of the SWAT model established a sound base for long-term management and planning of water resources at a provincial scale, where the dynamics of the water, food, and energy system will be examined next in greater detail.

Conflict of interest

All of the co-authors declare that there are no conflicts of interest.

Acknowledgements

Funding support from Alberta Innovates (grant # AI-EES 2077) is gratefully acknowledged. The authors are especially indebted to AEP, AAF, and other institutions within the GOA for their collaboration, provision of literature and data, and valuable comments and discussions related to this paper. We are especially grateful to Andy Jedrych, and Ted Harms from AAF for discussion of agricultural data.

Appendix A. Supplementary data

Supplementary data associated with this article can be found, in the online version, at http://dx.doi.org/10.1016/j.ejrh.2016.11.003.

References

AARD – Alberta Agriculture Rural Development, 2010. Agri-food statistics update, Alberta, Canada, Available at: http://www.agric.gov.ab.ca/$department/deptdocs.nsf/all/sdd13937/.

ABENV – Alberta Environment, 2007. Water for life: current and future water use in Alberta, Alberta, Canada ISBN: 978-0-7785-6797-4 724 pp., Available at: http://environment.gov.ab.ca/info/posting.asp?assetid=7935&categoryid=5/.

ABENV – Alberta Environment, 2008. Water for life: water supply assessment for Alberta, Alberta, Canada, ISBN: 978-0-7785-7660-0 111 pp., Available at: http://environment.gov.ab.ca/info/posting.asp?assetid=8393&categoryid=5/.

Abbaspour, K.C., Johnson, A., van Genuchten, M.T.H., 2004. Estimating uncertain flow and transport parameters using a sequential uncertainty fitting procedure. Vadose Zone J. 3, 1340–1352.

Abbaspour, K.C., Yang, J., Maximov, I., Sibe, R., Bogner, K., Mieleitner, J., Zobrist, J., Srinivasan, R., 2007. Modelling hydrology and water quality in the pre-alpine/alpine Thur watershed using SWAT. J. Hydrol. 333, 413–430, http://dx.doi.org/10.1016/j.jhydrol.2006.09.014.

Abbaspour, K.C., Rouholahnejad, E., Vaghefi, S., Srinivasan, R., Klöve, B., 2015. A continental-scale hydrology and water quality model for Europe: calibration and uncertainty of a high-resolution large-scale SWAT model. J. Hydrol. 524, 733–752, http://dx.doi.org/10.1016/j.jhydrol.2015.03.027.

Abbaspour, K.C., 2011. User Manual for SWAT-CUP: SWAT Calibration and Uncertainty Analysis Programs, Eawag. Swiss Fed Inst. of Aquatic Science and Technology http://www.eawag.ch/organization/abteilungen/siam/software/swat/index_EN/.

Adamowicz, W.L., Percy, D., Weber, M., 2010. Alberta's Water Resource Allocation and Management System: A Review of the Current Water Resource Allocation System in Alberta. Alberta Water Research Institute & Alberta Innovates Energy and Environment Solutions, Calgary (Available at:) http://www.seawa.ca/wp-content/uploads/2014/08/Albertas_Water_Resource_Allocation_and_Management_System.pdf.

Alcamo, J., Doll, P., Henrichs, T., Kaspar, F., Lehner, B., Rosh, T., Siebert, S., 2003. Development and testing of the WaterGAP 2 global model of water use and availability. Hydrol. Sci. J. 48 (3), 317–337, http://dx.doi.org/10.1623/hysj.48.3.317.45290.

Alcamo, J., Flörke, M., Märker, M., 2007. Future long-term changes in global water resources driven by socio-economic and climatic changes. Hydrol. Sci. J. 52, 247–275.

Allan, J.A., 1997. Virtual Water: A Long Term Solution for Water Short Middle Eastern Economies? Occasional Paper. SOAS Water Issues Group. King's College, UK.

Alley, W.M., 2006. Tracking U.S groundwater reserves for the future? Environ. Sci. Policy Sustain. Dev. 48 (3), 10–25, http://dx.doi.org/10.3200/ENVT.48.3.10-25.

Amon-Arma, F., Yiridoe, E., Ahmad, N.H.M., Hebb, D., Jamieson, R., Burton, D., Madani, A., 2013. Effect of nutrient management planning on crop yield, nitrate leaching and sediment loading in thomas brook watershed. Environ. Manag. 52, 1177–1191, http://dx.doi.org/10.1007/s00267-013-0148-z.

Arnold, J.G., Srinivasan, R., Muttiah, R.S., Williams, J.R., 1998. Large area hydrologic modeling and assessment–Part 1: Model development. J. Am. Water Resour. Assoc. 34, 73–89, http://dx.doi.org/10.1111/j.1752-1688.1998.tb05961.x.

Beck, L., Bernauer, T., 2011. How will combined changes in water demand and climate affect water availability in the Zambezi river basin? Glob. Environ. Change 21, 1061–1072, http://dx.doi.org/10.1016/j.gloenvcha.2011.04.001.

Beek, L.P.H., Wada, Y., Bierkens, M.F.P., 2011. Global monthly water stress: 1. Water balance and water availability. Water Resour. Res. 47, W07517, http://dx.doi.org/10.1029/2010WR009791.

Best, L.C., Lowry, C.S., 2014. Quantifying the potential effects of high-volume water extractions on water resources during natural gas development Marcellus Shale, NY. J. Hydrol.: Reg. Stud. 1, 1–16.

Chapagain, A.K., Hoekstra, A.Y., Savenije, H.H.G., 2006. Water saving through international trade of agricultural products. Hydrol. Earth Syst. Sci. 10, 455–468, http://dx.doi.org/10.5194/hess-10-455-2006.

Clark, M.P., Fan, Y., Lawrence, D.M., Adam, J.C., Bolster, D., Gochis, D.J., Hooper, R.P., Kumar, M., Leung, L.R., Mackay, D.S., Maxwell, R.M., Shen, C., Swenson, S.C., Zeng, X., 2015. Improving the representation of hydrologic processes in Earth System Models. Water Resour. Res. 51, 5929–5956, http://dx.doi.org/10.1002/2015WR017096.

Doll, P., 2009. Vulnerability to the impact of climate change on renewable groundwater resources: a global-scale assessment. Environ. Res. Lett. 4, 035006, http://dx.doi.org/10.1088/1748-9326/4/3/035006.

Eum, H., Yonas, D., Prowse, T., 2014. Uncertainty in modelling the hydrologic responses of a large watershed: a case study of the Athabasca River Basin Canada. Hydrol. Process. 28, 4272–4293, http://dx.doi.org/10.1002/hyp.10230.

Evenson, G.R., Golden, H.E., Lane, C.R., Amico, E.D., 2015. Geographically isolated wetlands and watershed hydrology: a modified model analysis. J. Hydrol. 529, 240–256, http://dx.doi.org/10.1016/j.jhydrol.2015.07.039.

FAO, 1998. Crop Evapotranspiration – Guidelines for Computing Crop Water Requirements, FAO Irrigation and Drainage Paper 0254-5284.

Falkenmark, M., Rockstrom, J., 2006. The new blue and green water paradigm: breaking new ground for water resources planning and management. J. Water Res. Plan. 132, 129–132, http://dx.doi.org/10.1061/(ASCE)0733-9496(2006)132:3(129).

Falkenmark, M., Lundqvist, J., Widstrand, C., 1989. Macro-scale water scarcity requires micro-scale approaches. Nat. Resour. Forum 13, 258–267.

Famiglietti, J.S., 2014. The global groundwater crisis. Nat. Clim. Change 4 (11), 945–948, http://dx.doi.org/10.1038/nclimate2425.

Faramarzi, M., Abbaspour, K.C., Yang, H., Schulin, R., 2009. Modelling blue and green water resources availability in Iran. Hydrol. Process. 23, 486–501, http://dx.doi.org/10.1002/hyp.7160.

Faramarzi, M., Yang, H., Mousavi, J., Schulin, R., Binder, R.C., Abbaspour, K.C., 2010a. Analysis of intra-country virtual water trade to alleviate water scarcity in Iran. Hydrol. Earth Syst. Sci. 14, 1417–1433, http://dx.doi.org/10.5194/hess-14-1417-2010.

Faramarzi, M., Abbaspour, K.C., Schulin, R., Yang, H., 2010b. Modeling wheat yield and crop water productivity in Iran: implications of agricultural water management for wheat production. Agric. Water Manag. 97 (11), 1861–1875, http://dx.doi.org/10.1016/j.agwat.2010.07.002.

Faramarzi, M., Abbaspour, K.C., Vaghefi, S.A., Farzaneh, M., Zehnder, A.J.B., Srinivasan, R., Yang, H., 2013. Modeling impacts of climate change on freshwater availability in Africa. J. Hydrol. 480, 85–101, http://dx.doi.org/10.1016/j.jhydrol.2012.12.016.

Faramarzi, M., Srinivasan, R., Iravani, M., Bladon, K., Abbaspour, K.C., Zehnder, A.J.B., Goss, G.G., 2015. Setting up a hydrological model of Alberta: data discrimination analyses prior to calibration. Environ. Model. Softw. 74, 48–65, http://dx.doi.org/10.1016/j.envsoft.2015.09.006.

Feketa, B.M., Vorosmarty, C.J., 2002. High-resolution fields of global runoff combining observed river discharge and simulated water balances. Glob. Biogeochem. Cycles 16, 1042, http://dx.doi.org/10.1029/1999GB001254.

Fu, C., James, A., Yao, H., 2014. SWAT-CS: revision and testing of SWAT for canadian shield catchments. J. Hydrol. 511, 719–735, http://dx.doi.org/10.1016/j.jhydrol.2014.02.023.

GOA–Government of Alberta, 2004. Alberta Fertilizer Guide, AGRI-FACTS: Practical Information for Alberta's Agriculture Industry, 16 pp. Available at: http://www1. agric.gov.ab.ca/$department/deptdocs.nsf/all/agdex3894/.

GOA – Government of Alberta, 2010. Water for Life: Facts about Water in Alberta. Edmonton, Alberta, Canada, ISBN: 978-0-7785-8970-9, 67pp. Available at: http://environment.gov.ab.ca/info/library/6364.pdf.

GOA – Government of Alberta, 2015. Highlights of the Alberta Economy 2015, Available at: http://www.albertacanada.com/files/albertacanada/SP-EH_highlightsABEconomyPresentation.pdf.

Gain, A.K., Giupponi, C., 2015. A dynamic assessment of water scarcity risk in the Lower Brahmaputra River Basin: an integrated approach. Ecol. Indic. 48, 120–131, http://dx.doi.org/10.1016/j.ecolind.2014.07.034.

Gassman, P.W., Reyes, M.R., Green, C.H., Arnold, J.G., 2007. The soil and water assessment tool: historical development, applications, and future research directions. Trans. ASABE 50, 12111250.

Gassman, P.W., Arnold, J.G., Srinivasan, R., Reyes, M., 2010. The worldwide use of the SWAT model: technical drivers, networking impacts, and simulation trends. In: Proceeding of 21 St Century Watershed Technology: Improving Water Quality and Environment, CD-Rom Proceedings, 21–24 February 2010, Costa Rica.

Golden, H.E., Lane, C.R., Amatya, D.M., Bandilla, K.W., Kiperwas, H.R., Knightes, C.D., Ssegane, H., 2014. Hydrologic connectivity between geographically isolated wetlands and surface water systems: a review of select modeling methods. Environ. Model. Softw. 53, 190–206, http://dx.doi.org/10.1016/j.envsoft.2013.12.004.

Graveline, N., Majone, B., Van Duinen, R., Ansink, E., 2014. Hydro-economic modeling of water scarcity under global change: an application to the Gaíllego river basin (Spain). Reg. Environ. Change 14, 119–132, http://dx.doi.org/10.1007/s10113-013-0472-0.

He, M., Hogue, T.S., 2012. Integrating hydrologic modeling and land use projections for evaluation of hydrologic response and regional water supply impacts in semi-arid environments. Environ. Earth Sci. 65, 1671–1685, http://dx.doi.org/10.1007/s12665-011-1144-3.

Hoekstra, A.Y., Mekonnen, M.M., Chapagain, A.K., Mathews, R.E., Richter, B.D., 2012. Global monthly water scarcity: blue water footprints versus blue water availability. PLoS One 7, e32688.
Intelligence Community Assessment (ICA), 2012. Global Water Security. U.S. Off. of the Dir. of Natl. Intel., Washington, D.C, pp. 1–30.
Islam, Z., Gan, T.Y., 2014. Effects of climate change on the surface-water management of the South Saskatchewan River Basin. J. Water Resour. Plan. ASCE 332, e342.
Jarvis, A., Reuter, H.I., Nelson, A., Guevara, E., 2008. Hole-filled SRTM for the Globe Version 4, the CGIAR-CSI SRTM 90 M Database. http://srtm.csi.cgiar.org.
Kiesel, J., Fohrer, N., Schmalz, B., White, M.J., 2010. Incorporating landscape depressions and tile drainages of a northern German lowland catchment into a semi-distributed model. Hydrol. Process. 24, 1472–1486, http://dx.doi.org/10.1002/hyp.7607.
Kijne, J.W., Barker, R., Molden, D., 2003. Water productivity in agriculture: limits and opportunities for improvement. Comprehensive Assessment of Water Management in Agriculture Series 1. CAB7IWMI, Wallingford, Colombo.
Krause, P., Boyle, D.P., Bäse, F., 2005. Comparison of different efficiency criteria for hydrological model assessment. Adv. Geosci. 5, 89–97, http://dx.doi.org/10.5194/adgeo-5-89-2005.
Lambin, E.F., Gibbs, H.K., Ferreira, L., Grau, R., Mayaux, P., Meyfroidt, P., Morton, D.C., Rudel, T.K., Gasparri, I., Munger, J., 2013. Estimating the world's potentially available cropland using a bottom-up approach. Glob. Environ. Change 23, 892–901, http://dx.doi.org/10.1016/j.gloenvcha.2013.05.005.
Lapp, S., St-Jacques, J.M., Sauchyn, D., Vanstone, J., 2013. Forcing of hydroclimatic variability in the northwestern Great Plains since 1406 CE. Quat. Int. 310, 47–61, http://dx.doi.org/10.1016/j.quaint.2012.09.011.
Lenzen, M., Moran, D., Bhaduri, A., Kanemoto, K., Bekchanov, M., Geschke, A., Foran, B., 2013. International trade of scarce water. Ecol. Econ. 94, 78–85, http://dx.doi.org/10.1016/j.ecolecon.2013.06.018.
Liu, J., Liu, Q., Yang, H., 2016. Assessing water scarcity by simultaneously considering environmental flow requirements, water quantity, and water quality. Ecol. Indic. 60, 434–441, http://dx.doi.org/10.1016/j.ecolind.2015.07.019.
Marshall, S.J., 2014. Meltwater runoff from haig glacier: canadian rocky mountains, 2002–2013. Hydrol. Earth Syst. Sci. 18, 5181–5200, http://dx.doi.org/10.5194/hess-18-5181-2014.
Mekonnen, M.M., Hoekstra, A.Y., 2010. A global and high-resolution assessment of the green, blue and grey water footprint of wheat. Hydrol. Earth Syst. Sci. 14, 1259–1276, http://dx.doi.org/10.5194/hess-14-1259-2010.
Molden, D., Murray-Rust, H., Sakthivadivel, R., Makin, I., 2003. A water productivity framework for understanding and action. In: Kijne, J.W., Barker, R., Molden, D. (Eds.), Water Productivity in Agriculture: Limits and Opportunities for Improvement. CABI Publishing, Wallingford, UK.
Mwale, D., Gan, T.Y., Devito, K., Mendoza, C., Silins, U., Petrone, R., 2009. Precipitation variability and its relationship to hydrologic variability in Alberta. Hydrol. Process. 23, 3040–3056, http://dx.doi.org/10.1002/hyp.7415.
Mwangi, H.M., Julich, S., Patil, S.D., McDonald, M.A., Feger, K., 2016. Relative contribution of landuse change and climate variability on discharge of upper Mara River, Kenya. J. Hydrol. Reg. Stud. 5, 244–260.
Nazemi, A., Wheater, H.S., 2015. On inclusion of water resource management in Earth system models- part 2: representation of water supply and allocation and opportunities for improved modeling. Hydrol. Earth Syst. Sci. 19, 63–90, http://dx.doi.org/10.5194/hess-19-63-2015.
Neitsch, S.L., Arnold, J.G., Kiniry, R.J., Williams, R.J., 2011. Soil and Water Assessment Tool Theoretical Documentation: Version 2009 TWRITR-191. Texas Water Resources Institute, Texas A&M University System, College Station, Texas, 77843-2118.
Neverre, N., Dumas, P., Nassopoulos, H., 2016. Large-scale water scarcity assessment under global changes: insights from a hydroeconomic framework. Hydrol. Earth Syst. Sci. Discuss. 2016, http://dx.doi.org/10.5194/hess-2015-502.
Oki, T., Kanae, S., 2006. Global hydrological cycles and world water resources. Science 313, 1068–1072, http://dx.doi.org/10.1126/science.1128845.
Pomeroy, J.W., Shook, K., Fang, X., Dumanski, S., Westbrook, C., Brown, T., 2014. Improving and Testing the Prairie Hydrological Model at Smith Creek Research Basin Research Report. Center for Hydrology University of Saskatchewan, 102 pp., Available at: http://www.usask.ca/hydrology/reports/CHRpt14_PHM_SCRB.pdf.
Rahbeh, M., Chanasyk, D., Miller, J., 2013. Modelling the effect of irrigation on the hydrological output from a small prairie watershed. Can. Water Resour. J. 38, 280–295, http://dx.doi.org/10.1080/07011784.2013.849856.
Raskin, P., Gleick, P., Kirshen, P., Pontius, G., Strzepek, K., 1997. Water futures: assessment of long-Range patterns and prospects. In: Background Document to the Comprehensive Assessment of the Freshwater Resources of the World Report. (WMO, 1997). Stockholm Environment Institute, Stockholm, Sweden.
Refsgaard, J.C., van der Sluijs, J.P., Højberg, A.L., Anrolleghem, P.A., 2007. Uncertainty in the environmental modelling process – A framework and guidance. Environ. Model. Softw. 22, 1543–1556, http://dx.doi.org/10.1016/j.envost.2007.02.004.
Richey, A.S., Thomas, B.F., Lo, M., Reager, J.T., Famiglietti, J.S., Voss, K., Swenson, S., Rodell, M., 2015. Quantifying renewable groundwater stress with GRACE. Water Resour. Res. 51 (7), 5217–5238, http://dx.doi.org/10.1002/2015WR017349.
Rijsberman, F.R., 2006. Water scarcity: fact or fiction? Agric. Water Manag. 80, 5–22, http://dx.doi.org/10.1016/j.agwat.2005.07.001.
Rouholahnejad, E., Abbaspour, K.C., Vejdani, M., Srinivasan, R., Schulin, R., Lehmann, A., 2012. Parallelization framework for calibration of hydrological models. Environ. Model. Softw. 31, 28–36.
Sauchyn, D.J., St-Jacques, J.M., Luckmanb, B.H., 2015. Long-term reliability of the Athabasca River (Alberta, Canada) as the water source for oil sands mining. Proc. Natl. Acad. Sci. U. S. A. 112 (41), 12621–12626, http://dx.doi.org/10.1073/pnas.1509726112.
Schierhorn, F., Faramarzi, M., Prishchepov, A.V., Koch, F.J., Müller, D., 2014. Quantifying yield gaps in wheat production in Russia. Environ. Res. Lett. 9, 084017, http://dx.doi.org/10.1088/1748-9326/9/8/084017.
Schuol, J., Abbaspour, K.C., Yang, H., Srinivasan, R., Zehnder, A.J.B., 2008. Modeling blue and green water availability in Africa. Water Resour. Res. 44, W07406, http://dx.doi.org/10.1029/2007WR006609.
Seckler, D., Amarasinghe, U., Molden, D., 1998. World Water Demand and Supply, 1990–2025: Scenarios and Issues Research Report 19. International Water Management Institute, Colombo, Sri Lanka.
Seidou, O., Ramsay, A., Nistor, I., 2012. Climate change impacts on extreme floods: combining imperfect deterministic simulations and non-stationary frequency analysis. Nat. Hazards 61, 647–659, http://dx.doi.org/10.1007/s11069-011-0052-x.
Shrestha, R.R., Dibike, Y.B., Prowse, T.D., 2012. Modeling Climate change impacts on hydrology and nutrient loading in the upper Assiniboine Catchment. J. Am. Water Resour. Assoc. 48 (1), 74–89, http://dx.doi.org/10.1111/j. 1752-1688.2011.00592.x.
Song, X., Zhang, J., Zhan, C., Xuan, Y., Ye, M., Xu, C., 2015. Global sensitivity analysis in hydrological modeling: review of concepts, methods, theoretical framework, and applications. J. Hydrol. 523, 739–757, http://dx.doi.org/10.1016/j.jhydrol.2015.02.013.
Sušnik, J., Vamvakeridou-Lyroudia, L.S., Savić, D.A., Kapelan, Z., 2012. Integrated System Dynamics Modelling for water scarcity assessment: case study of the Kairouan region. Sci. Total Environ. 440, 290–306, http://dx.doi.org/10.1016/j.scitotenv.2012.05.085.
Sullivan, C.A., Meigh, J.R., Giacomello, A.M., 2003. The water poverty index: development and application at the community scale. Nat. Resour. Forum 27, 189–199.
Talozi, S., Sakaji, Y.A., Altz-Stamm, A., 2015. Towards a water–energy–food nexus policy: realizing the blue and green virtual water of agriculture in Jordan. Int. J. Water Resour. D 31 (3), 461–482, http://dx.doi.org/10.1080/07900627.2015.1040544.
Tennant, D.L., 1976. Instream flow regimens for fish, wildlife, recreation and related environmental resources. Fisheries 1, 6–10.
Trion, M., Caya, D., 2014. Evaluating the SWAT's snow hydrology over a Northern Quebec watershed. Hydrol. Process. 28, 1858–1873, http://dx.doi.org/10.1002/hyp.9730.
UNEP – united Nation Environment Programme, 2011. Towards a Green Economy: Pathways to Sustainable Development and Poverty Eradication, Available at: http://www.unep.org/greeneconomy/AboutGEI/WhatisGEI/tabid/29784/Default.aspx.
Vörösmarty, C.J., Green, P., Salisbury, J., Lammers, R.B., 2000. Global water resources: vulnerability from climate change and population growth. Science 289 (5477), 284–288, http://dx.doi.org/10.1126/science.289.5477.284.

Vörösmarty, C.J., McIntyre, P.B., Gessner, M.O., Dudgeon, D., Prusevich, A., Green, P., Glidden, S., Bunn, S.E., Sullivan, C.A., Liermann, C.R., Davies, P.M., 2010. Global threats to human water security and river biodiversity. Nature 467, 555–561.

Vlotman, W.F., Ballard, C., 2014. Water, food and energy supply chains for a green economy. Irrig. Drain. 63, 232–240, http://dx.doi.org/10.1002/ird.1835.

Wada, Y., van Beek, L.P.H., Viviroli, D., Durr, H.H., Weingartner, R., Bierkens, M.F.P., 2011. Global monthly water stress: 2 Water demand and severity of water stress. Water Resour. Res. 47, W07518, http://dx.doi.org/10.1029/2010WR009792.

Wheater, H., Gober, P., 2013. Water security in the Canadian Prairies: science and management challenges. Philos. Trans. Ser. A: Math. Phys. Eng. Sci. 371, 20120409, http://dx.doi.org/10.1098/rsta.2012.0409.

World Economic Forum, 2015. Global Risks 2015: 10th Edition, Insight Report. Geneva, Switzerland, 65 pp., http://www.weforum.org/docs/WEF_Global_Risks_2015_Report15.pdf.

Yang, H., Wang, L., Abbaspour, K.C., Zehnder, A.J.B., 2006. Virtual water trade: an assessment of water use efficiency in the international food trade. Hydrol. Earth Syst. Sci. 10, 443–454, http://dx.doi.org/10.5194/hess-10-443-2006.

Yang, W., Wang, X., Liu, Y., Gabor, S., Boychuk, L., Badiou, P., 2010. Simulated environmental effects of wetland restoration scenarios in a typical Canadian prairie watersheds. Wetl. Ecol. Manag. 18, 269–279, http://dx.doi.org/10.1007/s11273-009-9168-0.

Zeitoun, M., Allan, J.A.T., Mohieldeen, Y., 2010. Virtual water 'flows' of the Nile Basin, 1998–2004: A first approximation and implications for water security. Glob. Environ. Change 20, 229–242, http://dx.doi.org/10.1016/j.gloenvcha.2009.11.003.